Cooperative folding of muscle myosins: I. Mechanical model

Matthieu Caruel, Jean-Marc Allain, Lev Truskinovsky

Cooperative folding of muscle myosins: I. Mechanical model.

M. Caruel,[1] J.-M. Allain,[2] and L. Truskinovsky[2,*]

[1] *Inria, 1 rue Honoré d'Estienne d'Orves, 91120 Palaiseau, France*
[2] *LMS, CNRS-UMR 7649, Ecole Polytechnique, 91128 Palaiseau, France*

(Dated: December 2, 2013)

Mechanically induced folding of passive cross-linkers is a fundamental biological phenomenon. A typical example is a conformational change in myosin II responsible for the power-stroke in skeletal muscles. In this paper we present an athermal perspective on such folding by analyzing the simplest purely mechanical prototype: a parallel bundle of bi-stable units attached to a common backbone. We show that in this analytically transparent model, characterized by a rugged energy landscape, the ground states are always highly coherent, single-phase configurations. We argue that such cooperative behavior, ensuring collective conformational change, is due to the dominance of long-range interactions making the system non-additive. The detailed predictions of our model are in agreement with experimentally observed non-equivalence of fast force recovery in skeletal muscles loaded in soft and hard devices. Some features displayed by the model are also recognizable in the behavior of other biological systems with passive multi-stability and long-range interactions including detaching adhesive binders and pulled RNA/DNA hairpins.

I. INTRODUCTION

Recently, considerable attention has been focussed on the study of *mechanical* behavior of cells and tissues. These living systems are viewed as prototypes of new biologically inspired materials that can actively generate stresses and modify their rheological properties. They can also accommodate loading through active remodeling and growth. This intriguing mechanical behavior is associated with dominant hierarchical structures encompassing broad ranges of scales that are linked by complex energy cascades [1–3]. In contrast to conventional materials, distributed biological systems are driven intrinsically and incorporate mechanisms that produce energy and maintain disequilibrium [4, 5].

While the challenge of finding sufficiently general principles governing the mechanical behavior of active systems remains elusive, our understanding of specific biological regimes and mechanisms has been considerably improved in recent years. An important example of a living system, whose functioning is reasonably well understood on both anatomical and bio-chemical levels, is a skeletal (striated) muscle [6, 7]. A narrow functionality of this system is behind its relatively simple, almost crystalline geometry which suggests the study of a single representative unit (half-sarcomere). The fact that this unit has a quasi-one-dimensional structure makes it a natural choice for a systematic mechanical modeling. Among many functional regimes involving this unit, the first candidate for a detailed study is the fast force re-generation after abrupt shortening. The implied force recovery is a passive phenomenon that is not ATP driven and can be therefore studied in a purely mechanical framework.

From structural reconstructions we know that behind the fast force recovery is the *power-stroke*: a mechanically induced folding of myosin cross-bridges attached to actin filaments. Similar mechanism are responsible for a variety of biological phenomena from unzipping of single bio-molecules to contraction of cytoskeleton.

In this paper, we study the *athermal* mechanics of the load-induced muscle power-stroke triggered by force/length increments. An elementary contractile unit (half-sarcomere) is represented by a parallel bundle of myosin cross-bridges attached to a common rigid "backbone". We reassess the classical Huxley and Simmons (HS) model of fast force recovery in skeletal muscles by assuming that each cross-bridge is a hard spin unit coupled to a harmonic spring and propose a regularized version of this model were hard spins are replaced by soft spins exhibiting continuous conformational change. We then deviate from the HS scheme and incorporate filament elasticity in the form of a crucial mean-field interaction between individual cross-bridges. The ensuing mechanical system is characterized by a rugged energy landscape with multiple metastable states describing mixed pre- and post-power-stroke configurations. The ground states, however, are always associated with coherent, single phase configurations. We show that the implied *cooperative behavior* is due to the dominance of long-range interactions making the system non-additive and preventing the formation of mixed configurations. As we discuss at the end of the paper, in view of the prototypical nature of the model, these general conclusions pertain to a variety of other biological systems with elastic interactions mediated by effective "backbones".

Below we discuss in more details the motivation and the main results of this work and the two accompanying papers [8, 9].

* trusk@lms.polytechnique.fr

A. Experimental background

Skeletal muscle is formed by a hierarchical system of fibers. At the micrometer scale individual myofibrils can be viewed as a periodic arrangement of contractile units called *sarcomeres*, however, the actual mechanism of muscle contraction resides in nano-scale interactions between actin and myosin filaments, see Fig. 1(a). More precisely, each sarcomere contains a sub-structure of (thin) actin filaments interacting with a complimentary sub-structure of (thick) myosin filaments. Myosin filaments are tight bundles of the joined tails of myosin II molecules which terminate with protruding nanometer-sized heads. The heads contain motor domains that can *actively* cross-link myosin and actin filamental substructures by forming intermittently stable *cross-bridges*, see Fig. 1(a). An elementary contractile unit is formed by ~ 100 cross-bridges connected in parallel, see the insert in Fig. 1(b).

According to the leading "sliding filament" hypothesis [10], attached cross-bridges generate force through a rapid conformational change known as the *power-stroke*. In order to recharge the power-stroke mechanisms the myosin heads must detach from actin binding sites and this can be accomplished only in the presence of ATP. The re-cocked cross-bridges reattach and the power-stroke mechanism strikes again. The collective cyclic action of the cross-bridges induces continuous relative sliding of actin and myosin filaments. This leads to the shortening of individual sarcomeres inducing macroscopic contraction [11, 12].

The attachment-detachment process is inseparable from the power-stroke in the acto-myosin autocatalytic cycle [13]. The individual kinetic steps, however, have vastly different characteristic times [14]. The power-stroke, taking place at a ~ 1 ms time scale, is the fastest step and it is commonly believed to be independent of the ATP activity which takes place on a 30 ms time scale [14, 15]. In view of this separation of time scales, the *passive* folding-unfolding of the myosin heads can be studied under the assumption that the cross-bridges remain attached. To this end, special experimental protocols have been designed which involve abrupt loading targeting the millisecond time scale [16].

The fast response of a tetanized muscle fiber to an abrupt length change imposed in a hard device (displacement clamp, isometric test) was first systematically studied in the pioneering paper of Huxley and Simmons [17]. The relaxation process was shown to be comprised of two phases; see Fig. 2 (a). The first phase corresponds to an elastic shortening during which the muscle tension drops in proportion to the applied length step to a level usually denoted by T_1. During the second phase, taking place at constant length and known as the *fast force recovery*, tension raises to a higher level usually denoted by $T_2 > T_1$. The value of T_2 is still strictly lower than the original tension $T_2 < T_0$, see Fig. 2(a). The full recovery of the force takes place during the third phase at a much longer time scale (~ 100 ms). This phase engages an active process driven by ATP hydrolysis which places this phenomenon outside a theory of passive behavior.

Similar experiments have been also performed in a soft device (load clamp, isotonic test) [20–22]. The initial response to a sudden force drop was shown to exhibit the same two phases, with sequential shortening first to the level δz_1 interpreted as an instantaneous elastic deformation, and then to the level δz_2 with the second process taking place at a fixed load, see Fig. 2 (b). At longer time scales, muscle subjected to fixed load enters a regime of isotonic shortening which is an active process laying again outside the scope of this study.

Denote by δz the applied displacement increment in the isometric test (hard device). Then, the function $T_1(\delta z)$ describes the force-elongation relation associated with instantaneous elastic deformation at a frozen conformational degrees of freedom, while the function $T_2(\delta z)$ can be interpreted as characterizing phase equilibrium of the attached cross-bridges, namely an internal redistribution of the myosin heads between the pre- and post-power-stroke conformations. Similarly, if $T - T_0$ is a force increment applied in an isotonic test (soft device), we assume that the function $\delta z_1(T)$ represents a frozen elastic response while the function $\delta z_2(T)$ describes the subsequent phase equilibration.

The force-elongation relations associated with both frozen and annealed responses have been thoroughly studied, see Fig. 3 (a). As we see, the relations $T_1(\delta z)$ and $\delta z_1(T)$ fully overlap, which means that the (almost linear) elastic response is identical in soft and hard devices. The equilibrium responses, characterized by the functions $T_2(\delta z)$ and $\delta z_2(T)$, also overlap except for a strip marked in gray in Fig. 3 (a) where the response observed in a hard device could not be reproduced in a soft device forming a distinct *gap* in the equilibrium data. Instead, damped coherent oscillations (hopping) with a period of about 30 ms were reported [21, 23–26].

We notice that the force-elongation relation recorded for the gap parameters in the hard device experiments is highly nonlinear exhibiting an extended plateau where equilibrium force is practically independent of the elongation. Such plateau is biologically advantageous because the system is able to quickly accommodate small external length perturbations while maintaining the same level of force. The overall two-stage mechanical response to the abrupt loading observed in both types of experiments is reminiscent of Maxwell visco-elasticity, however, it is clear that it cannot be reproduced by a standard linear visco-elastic model.

The *non-equivalence* of the equilibrium responses in isotonic and isometric experiments suggests that the underlying distributed (multi-element) mechanical system behaves differently in soft and hard devices. The disparity between the data obtained in these types of tests becomes even more pronounced if we also consider kinetics. Thus, our Fig. 3 (b) shows that the rate of fast force (length) recovery, interpreted as the inverse of the

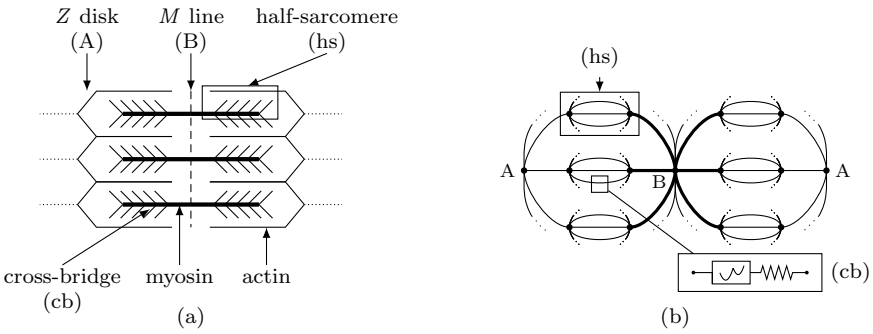

FIG. 1. (a) anatomical structure of a myofibril segment of periodicity showing force generating half-sarcomeres (hs) connected (passively cross-linked) by Z disks (A) and M lines (B). Each half-sarcomere includes an actin (thin) filament interacting with a myosin (thick) filament through a parallel bundle of attaching and detaching cross-bridges (cb); (b) topological structure of the same myofibril emphasizing dominance of long-range interactions. The inset shows the basic mechanical structure of an individual cross-bridge.

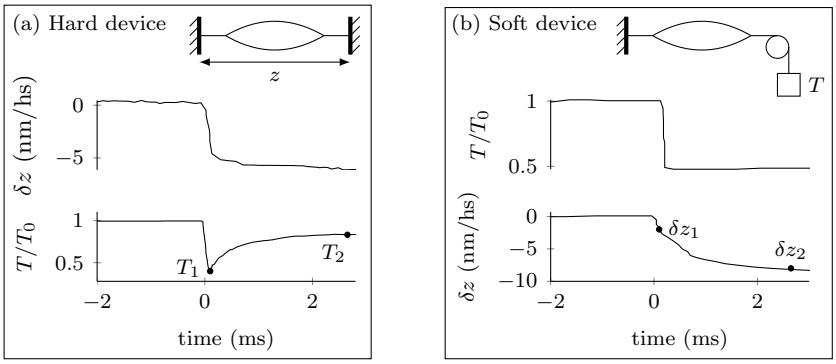

FIG. 2. Quick recovery experiments. (a) hard device where the average half-sarcomere (hs) length z is controlled. Upper trace, elongation step applied to the sample; bottom trace, tension response where t_1 and t_2 at the end of phase 1 and phase 2, respectively, are indicated. (b) soft device where the average half-sarcomere (hs) tension t is controlled. Upper trace, force step applied to the sample; bottom trace, elongation response with indicated shortening δz_1 and δz_2 at the end of phase 1 and phase 2, respectively. Data from [18] for (a) and from [19] for (b).

time separating the elastic and equilibrium phases of the response, is considerably lower in a soft device than in a hard device. This peculiarity of the passive behavior of skeletal muscles, implying that the response in soft device may be of a two-stage type with the formation of intermediate long living quasi-equilibrium states, was noticed experimentally [19, 22, 27], but remained unexplained.

B. Theoretical approaches

Our theoretical understanding of *active* force generation in skeletal muscles is mostly based on chemo-mechanical models involving fitting functions [10, 14, 33–37]. These phenomenological models have been recently complemented by the *mechanistic descriptions* interpreting muscle contraction as continuous stochastic dynamics in a complex energy landscape [38–41]. In this paper, we adopt the mechanistic approach and extend it to the study of the puzzling aspects of passive responses displayed by skeletal muscles exposed to abrupt loading.

The interpretation of fast force recovery as an *equilibration* of two bound conformational states of myosin motors, representing pre- and post-power-stroke configurations, goes back to Huxley and Simmons [17]. They developed a mechanistic model (HS model) where the two conformations were described as discrete chemical species. These spin-type states were then extended as one dimensional manifolds parameterized by the stretch of a series elastic spring. In this paper we interpret this model as a spin system coupled to an elastic element which is a rather typical physical situations with applications ranging from Jahn-Teller effect and ripples in graphene sheets to unzipping of biological macromolecules [42–44]. Huxley and Simmons computed equilibrium properties of this system at finite temperature and approximated kinetics by a Kramers type reaction equation built on some natural phenomenological assumptions regarding the force dependence of the energy barrier separating the two conformational states. In about the same time somewhat similar ideas were developed in the closely related theory of bi-stable adhesion clusters [45].

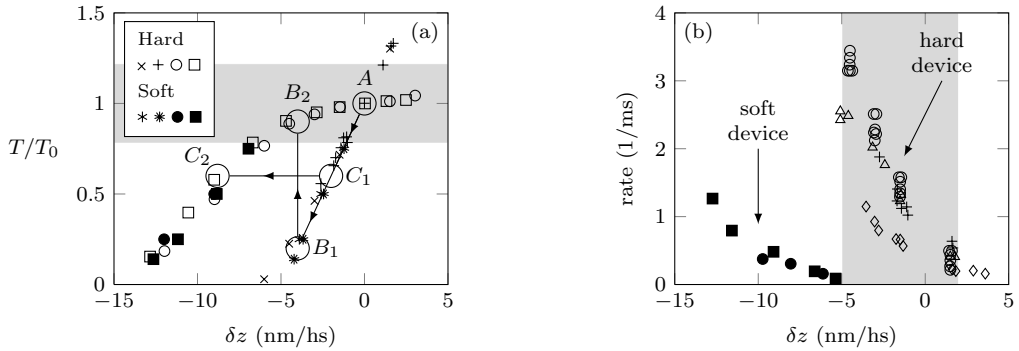

FIG. 3. Results of fast force (length) recovery experiments collected from different references. (a) tension and elongation at the end of phase 1 (cross and stars) and phase 2 (shaped symbols) with soft device shortening indicated by filled symbols; (b) rate of the quick recovery process in a hard (open symbols) and in a soft (filled symbols) device: we juxtapose the kinetics of the systems following the two different pathways between the same initial and final states, namely $T = T_0,\ \delta z = 0\,(A)$, and $T = T_2\,(B_2), \delta z = \delta z_2\,(C_2)$. The gray region shows the gap domain where the quick recovery is not observed in a soft device. Origin of the data: $\diamond$ from [17], $\times\,\circ$ from [28], $\triangle$ from [29], $*\,\bullet$ from [19], $*\,\blacksquare$ from [30].

The HS model was later extended as a more general chemo-mechanical model by Hill [46, 47] and this theoretical approach to the description of both passive and active responses of skeletal muscles has become broadly accepted [14, 36, 37, 41, 48]. Based on important insight from [49] the hard spin model was later generalized as a soft spin model [50, 51]. This allowed the authors to replace jump processes by a continuous stochastic dynamics in a landscape with clearly specified barriers and to bring closer the chemo-mechanical modeling and the description in terms of Brownian ratchets. None of the above papers, however, addressed the observed peculiarities of passive response including the *non-equivalence* of fast recovery in hard and soft devices. In particular, neither the gap in the equilibrium isotonic data nor the difference of kinetics in isotonic and isometric protocols has been previously rationalized.

In this series of papers we provide a compelling evidence that the difference between the passive responses of skeletal muscles in hard and soft devices is a result of the dominance of *long-range interactions* in muscle architecture. A quick look at the topological structure of the muscle acto-myosin network, see Fig. 1 (b), clearly shows that parallel mechanical connections are present at different scales. This special structure, where interactions are transmitted through a system of "backbones", makes muscle tissue mechanically different from the conventional materials where the dominant interactions are of short range nature.

The peculiar mechanical behavior of muscle cells is shared by generic elastically bound hierarchical biological structures/networks with unfolding passive cross-linkers [52–55]. In order to explain this behavior one needs to account for the *cooperative* folding-unfolding of individual multi-stable units and we show that such cooperativity is already recognizable in the simplest athermal setting ignoring the presence of ATP. A study of such minimal models may be the best way to make explicit the link between the coherent response and the dominance of multiple shared links. This internal architecture leads to a *mean-field* type feedback which has been long known as the source of cooperative behavior not only in biological but also in social systems [56, 57].

C. Summary of the results

As we have already mentioned, we base our conclusions on the study of a prototypical model. The starting point is a representation of a half-sarcomere as a set of N cross-bridges connected in *parallel*. This is the simplest architecture compatible with the idea of a mean-field coupling. If we interpret a single cross-bridge as a spin unit linked to a series spring, we obtain the HS model [17]. Huxley and Simmons studied the behavior of their model only in a hard device and at finite temperature they did not observe any cooperative effects. Our analysis shows that the HS model is degenerate in a hard device and explains why at finite temperature the collective behavior in the HS setting can be expected only in a soft device.

To obtain a broader picture we regularize the HS model in two important ways. First, following [50] we replace the discrete chemical states (hard spin model) by a continuous double-well potential with a finite energy barrier (soft spin model). This regularization, however, turns out to be insufficient to capture the collective behavior in a hard device and one also needs to take into consideration the elastic interaction between individual cross-bridges due to filament elasticity [58–60]. The simplest way to capture such interaction is to load the parallel bundle of the attached cross-bridges through a series spring which can be then viewed as a lump description of filament elasticity. This additional regularization introduces the desired mean-field coupling in a hard device and opens the way towards obtaining not only qualitative but also quantitative agreement with experimental data obtained

in both isometric and isotonic loading conditions. Our systematic comparison of the mechanical behavior displayed by the HS and the RHS (regularized HS) models shows that the proposed additions to the HS model are irreducible.

The present paper (referred in the sequel as Paper I) is the first in a series of three communications. In Paper I we compare the equilibrium responses of the HS and the RHS models at zero temperature. In Paper II [9] we extend the analysis to finite temperatures. Paper III [8] deals with kinetic (transient) response of the RHS model, contains parameter fitting and offers a detailed quantitative comparison with available experimental data on skeletal muscles.

More specifically, in Paper I we show that a salient feature of the purely mechanical (zero temperature) energy landscape for both HS and RHS models is the association of the ground states exclusively with the macroscopic energy wells corresponding to *coherent* configurations. In those states the cross-bridges are all either in pre- or in post-power-stroke states. An explicit construction also shows that in both models the coherent states are separated by a rugged energy landscape describing multiple metastable configurations. In the continuum (thermodynamic) limit the set of metastable states becomes dense allowing for a hysteretic behavior.

We show, however, that in the HS model the cooperative power-stroke is robust only in a soft device while in a hard device it can be qualified as "fragile". By this we imply that the height of the energy barrier between the coherent states is finite in a soft device, where the cross-bridges do interact, and is equal to zero in the degenerate case of a hard device, where the cross-bridges do not interact. As a result, in the isometric zero temperature tests, one can expect to see incoherent unfolding of individual cross-bridges while in similar isotonic conditions the unfolding must be necessarily collective. It is then not surprising that at finite temperatures the coherent states in the HS model completely disappear when the loading is isometric and while persisting when it is isotonic, see [8].

In the RHS model the collective behavior is robust in both types of tests, however, the energy barriers separating the coherent states are markedly higher in a soft device than in a hard device which is fully compatible with kinetic data. More specifically, the computed difference in height of the energy barriers explains the retarded relaxation in isotonic experiments and justifies the recorded gap in equilibrium data. The analytical transparency of the model at zero temperature allowed us to trace the origin of this unusual kinetic behavior directly to mean-field interactions imposed by a common backbone.

Another manifestation of the non-equivalence of soft and hard devices, which for both HS and RHS models persists even in the continuum limit, is that the homogenized stiffness can become negative in the hard but not in a soft device. In other words, the relaxed potential, representing the global minimum of the energy, is always convex in a soft device but is only convex-concave in a hard device. The non-convexity of the ground state energy in a hard device means that the system cannot be relaxed by creating configurations with both folded and unfolded units because of the high elastic energy of the mixing. Such *meta-material* response [61], contradicts the conventional intuition about the material behavior in systems with short-range interactions. We show that this behavior is a direct result of the dominance of mean-field elastic coupling and the ensuing non-additivity of the energy. Interestingly, the fact that long-range interactions can lead to negative equilibrium susceptibility has been long known, for instance, in the theory of self-gravitating systems [62].

In view of the prototypical nature of the proposed model, the approach developed in this paper can be used in the study of other biological systems with long-range interactions. In particular, it describes the passive behavior of adhesive binders where individual elements also interact through a common elastic background and therefore exhibit cooperative de-bonding [63–66]. Similar mechanical behavior is also associated with the mechanical denaturation of RNA and DNA hairpins exposed to various types of applied mechanical loadings imposed through elastic "handles". Here the effective backbone is present due to the prevalence of stem-loop structures and the macroscopic bi-stability manifests itself through a cooperative hopping between folded and unfolded configurations [42, 44, 67]. Further examples of molecular systems exhibiting similar collective folding-unfolding behavior associated with the dominance of long-range elastic interactions are provided by protein β-hairpins [68] and coiled coils [69].

The paper is organized as follows. In Section II, we study the equilibrium mechanical behavior in the classical HS setting and show that already in this minimal model the behavior in soft and hard devices is different. The RHS model is introduced in Section III where we demonstrate how it removes the degeneracies of the HS model and effectively interpolates between the soft and hard device behaviors. The last Section IV contains the discussion of the results and our conclusions.

Some preliminary results of this work have been briefly announced in [70]

II. THE HS MODEL

Consider the behavior of an elementary contractile unit of a striated muscle, a half-sarcomere, containing one actin filament and one myosin filament cross-linked by N cross-bridges. In the HS model [17] each cross-bridge is represented by a bistable potential connected to a series spring. The potential representing two folding configurations of the head domain bound to the actin filament was assumed to have infinitely narrow energy wells representing two chemical states. This is essentially a spin-based description where each spin unit is coupled with a har-

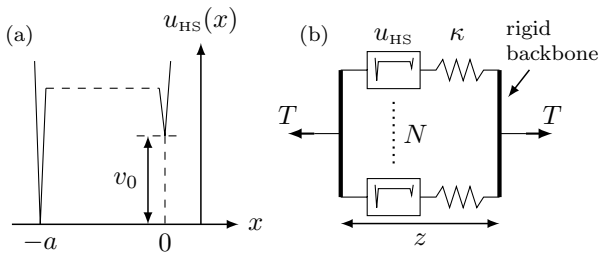

FIG. 4. Our interpretation of the HS model of a half-sarcomere [17]. (a) energy landscape of the head; (b) schematic of a half-sarcomere containing N cross-bridges in a soft device.

monic elastic element (oscillator), see Fig. 4.

The potential describing a single spin units can be written in the form

$$u_{\rm HS}(x) = \begin{cases} v_0 & \text{if } x = 0, \\ 0 & \text{if } x = -a. \end{cases} \tag{1}$$

Here the spin variable x takes two values associated with two chemical states, namely 0 and $-a$ which corresponds to the pre- and the post-power-stroke, respectively. By a we denoted the "reference" size of the power-stroke interpreted as the distance between two infinitely localized energy wells with the pre-power-stroke state we associate an energy level v_0 while the post-power-stroke is considered a ground state with zero energy. The potential (1) is shown schematically in Fig. 4(a).

In addition to a spin unit with energy (1) each cross-bridge contains a linear shear spring with stiffness κ; see Fig. 4(b). The energy of the elastic spring is

$$u(x) = \frac{\kappa}{2}x^2$$

and the energy of the whole cross-bridge is

$$u_{cb} = u_{HS}(x) + u(z - x). \tag{2}$$

Without loss of generality, we can assume that the rest length of the linear spring is already incorporated into the definition of the elongation z so that z is the total elongation relative to the rest length. The variable z is then an external continuous degree of freedom while the variables x is a discrete internal degree of freedom.

The behavior of a mechanical system with energy (2) is non-trivial in the sense that it has a multi-stable response. Indeed, consider an individual cross-bridge in a hard device (at a given elongation z). The equilibrium state is obtained by solving the equation $u'_{\rm HS}(x) = z - x$. At each value of z there are two solutions, $\overline{x}_1 = -1$ and $\overline{x}_0 = 0$, and as a consequence, the system can exhibit two different tension levels. The mechanical behavior an individual cross-bridge is illustrated in Fig. 5 where the arrows show a schematic response to sudden shortening including a frozen elastic phase ($A \to B_1$) and a subsequent phase equilibration ($B_1 \to B_2$).

Consider now N attached cross-bridges. Their geometric configuration in a half-sarcomere is such that in the absence of filament elasticity these elements can be viewed as arranged in parallel, see Fig. 1(b). By making here an assumption that the backbone is rigid we neglected the inhomogeneities in the filaments and an additional coupling between the cross-bridges [58, 71] which will play an important role in the RHS model.

To non-dimensionalize the resulting model, which we associate with the names of Huxley and Simmons (HS model) even though they never considered such parallel connection explicitly (for this representation, see [50]), we choose a as a characteristic distance, associate the characteristic energy scale with κa^2 and normalize forces by κa. Then the only remaining dimensionless parameter of the model is $N \sim 100$ and we can write the total energy of the system (per cross-bridge) in the form

$$v(\boldsymbol{x}; z) = \frac{1}{N}\sum_{i=1}^{N}\left[(1 + x_i)\, v_0 + \frac{1}{2}(z - x_i)^2\right]. \tag{3}$$

Here, for convenience, we dropped the signs identifying non-dimensional quantities.

Assume first that the system is placed in a hard device where the total elongation z is prescribed. In this setting each cross-bridge is exposed to the same total elongation z while individual units are independent. This is the reason why Huxley and Simmons, who only dealt in their classical paper [17] only with isometric loading, did not have to consider the parallel bundling explicitly and could perform their analysis while dealing only with one cross-bridge. As we are going to see later, the price of this simplification is the omission of the important collective effects.

In a soft device, which was not considered in the original paper of Huxley and Simmons [17], the prescribed control parameter is the total tension T. Then the energy per cross-bridge characterizing such system can be written as

$$w(\boldsymbol{x}, z; t) = \frac{1}{N}\sum_{i=1}^{N}\left[(1 + x_i)\, v_0 + \frac{1}{2}(z - x_i)^2\right] - tz, \tag{4}$$

where $t = T/N$ is the force per cross-bridge. Now for each cross-bridge both x_i and z are internal degrees of freedom and the individual units can no longer be considered as independent. Indeed, if we minimize out the global continuous variable z, we see that the energy depends quadratically on $\sum_{i=1}^{N} x_i$. This introduces a mean-field interaction of infinitely long-range type among cross-bridges which is ultimately responsible for the cooperative behavior. Similar abstract system involving a mean-field interaction of Ising spins with a linear spring has been recently considered in [44] who suggested interesting applications of such models to force induced unzipping of biological macromolecules.

In the next two subsections we consider more systematically the mechanical behavior of N parallel cross-bridges in hard and soft devices.

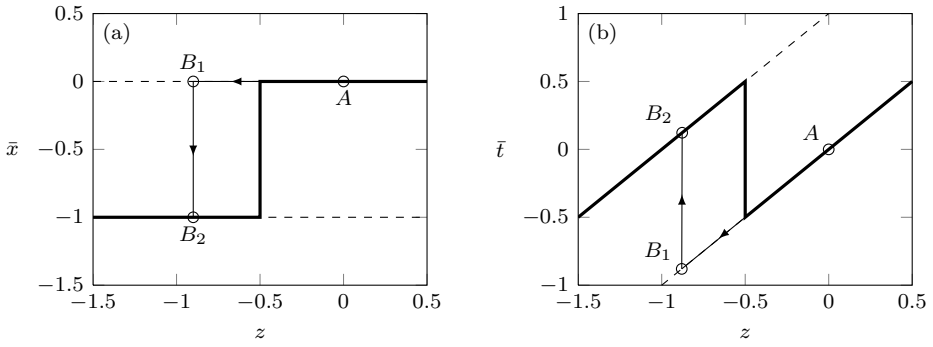

FIG. 5. Properties of a single power-stroke element with the HS model. (a) equilibrium positions for various z; (b) corresponding tension levels. Solid lines, metastable states; bold line, global minimum. Parameters are $\kappa = 1$ and $v_0 = 0$.

A. Hard device

To find the equilibrium response of the HS model in a hard device we need to solve the following system of equilibrium equations

$$\left.\frac{\partial}{\partial x_i}\right|_{z,\{x_{j\neq i}\}} v = 0 \text{ for all } 1 \leq i \leq N. \tag{5}$$

Since the cross-bridges do not interact, each one can be considered separately and therefore, as we have already seen, Eq. 5 has two solutions for each i independently of the loading z; $\hat{x}_0 = 0$, corresponding to the *pre-power-stroke* conformation and $\hat{x}_1 = -1$, corresponding to the *post-power-stroke* conformation. A given equilibrium state is then characterized by the distribution of the N cross-bridges between these two spin configurations. Due to the permutational invariance of the problem, each equilibrium state is fully characterized by a discrete "order parameter"

$$p = \frac{1}{N}\sum_{i=1}^{N} \alpha_i,$$

where $\alpha_i = 1$ if $x_i = \hat{x}_1 = -1$ and $\alpha_i = 0$ if $x_i = \hat{x}_0 = 0$. It represents the fraction of cross-bridges in the post-power-stroke state and becomes a continuous internal variable defined on $[0, 1]$ in the thermodynamic (continuous) limit $N \to \infty$.

In A we show that all solutions of (5) are metastable equilibria in the sense that they represent local minima of the energy (3). At a given value of the order parameter p, the energies of the corresponding metastable states are the same and are equal to

$$\hat{v}(z, p) = p\frac{1}{2}(z+1)^2 + (1-p)\big(\frac{1}{2}z^2 + v_0\big). \tag{6}$$

We observe that this energy is a simple linear combination of the energies of two limiting configurations, one with $p = 1$ and the energy $\frac{1}{2}(z+1)^2$ and the other one with $p = 0$, and the energy $\frac{1}{2}z^2 + v_0$. The absence of *mixing* is a manifestation of the fact that the two coexisting populations of cross-bridges, of pre- and post-power-stroke kind, do not interact in the case of a hard device loading.

The tension-elongation relations along metastable branches parameterized by p can be obtained from Eq. 6 by differentiation with respect to the loading parameter,

$$\hat{t}(z, p) = \frac{\partial}{\partial z}\hat{v}(z, p) = p\,(z+1) + (1-p)z = z + p. \tag{7}$$

One can see that at fixed p, the tension-elongation relations are equidistant parallel straight lines.

In the thermodynamic limit $N \to \infty$, we obtain a *dense* set of metastable configurations. They are infinitely close to each other and are separated by infinitely small barriers, see our Fig. 14(b). This is a typical situation when a mechanical system exhibits macroscopic hysteretic behavior with the most prominent examples in the theories of friction, plasticity and shape memory behavior [72]. A peculiar feature of the HS model is that the domain of hysteretic behavior extends indefinitely because the spin system does not have any stress thresholds.

To find the global minimum of the energy we need to perform at each value of z an additional minimizing over the discrete variable p. Since the energy is a linear function of p the global minimum is always located on the boundary of the admissible domain, either at $p = 0$ or $p = 1$. This means that the states with a mixed population of cross-bridges in pre- and post-power-stroke states are never globally stable. More specifically, if we compute the derivative

$$\frac{\partial}{\partial p}\hat{v}(z, p) = z + \frac{1}{2} - v_0.$$

we obtain that the configuration with the minimal energy is in fully in the pre-power-stroke state for $z > z_*$ and is in fully post-power-stroke state for $z < z_*$ where $z_* = v_0 - 1/2$. Although such response can be characterized as highly synchronized, we shall see in what follows that such coherent states are "fragile" artifacts of the degenerate HS setting that immediately disappear in both regularized and thermal models.

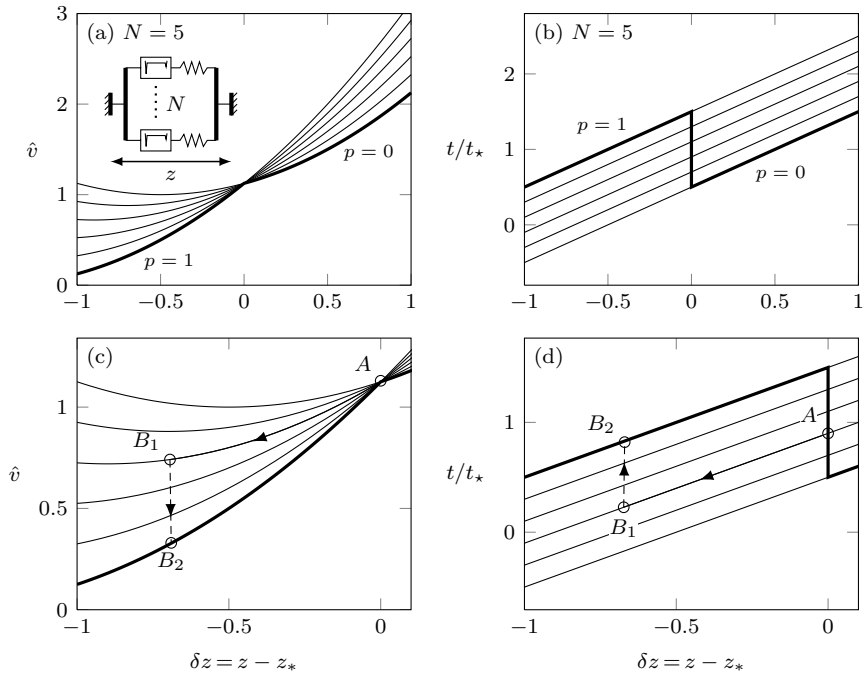

FIG. 6. Mechanical response of the HS model in a hard device with $N = 5$. (a) Energy levels of the metastable states ($p = 0, \frac{1}{5}, \ldots, 1$) for different applied elongations. (b) corresponding tension-elongation relations. (c) and (d) are details of (a) and (b) with an illustrated response path to fast loading experiment including the frozen elastic phase ($A \to B_1$) followed by the subsequent phase equilibration ($B_1 \to B_2$). Thick lines, global minimum corresponding to $p = 0$ (resp. $p = 1$) for $z > z_*$ (resp. $z < z_*$) . Parameters are, $v_0 = 1$ and $N = 5$.

To illustrate this general picture, we show in Fig. 6(a,b) the energy of the metastable states and the corresponding tension-elongation relations for the system with $N = 5$. In Fig. 6(c,d) we show the blow up near the initial state with $T = T_0$ (see A) where the arrows illustrate a schematic response of the system to sudden shortening including the frozen elastic phase with the initial value of the order parameter p fixed ($A \to B_1$) followed by the subsequent phase equilibration when the discrete variable p assumes the value corresponding to the global minimum of the energy ($B_1 \to B_2$). In the continuum limit $N \to \infty$ the system would look similar with the global minimum branches remaining unaffected and the set of local minima filling smoothly the whole domain of hysteretic behavior. The global minimum energy profile exhibits a characteristic kink near the crossing (folding) point. Similar kinks associated with unfolding of hairpins and other folding patterns have been observed in the energy profiles reconstructed from single molecule force spectroscopy measurements of proteins and nucleic acids [43].

One feature of the emerging picture is unusual given our experience with systems exhibiting mostly short range interactions. First, we notice that the relaxed energy corresponding to the path of global minimization is *nonconvex* independently of the number of units. This means that the energy is not getting convexified by the formation of mixtures as in systems with short range interactions (see, for instance, [73]) because the system is non-additive and all mixed states are energetically unfavorable due to high cost of mixing. This situation, however, is reminiscent of the one in the theory of elastic phase transitions where the relaxed energy is also nonconvex in the general case (it is only quasi-convex) which is again the consequence of long-range interactions exemplified in elasticity by the gradient constraint on the order parameter (see, for instance, [74]).

An interesting consequence of the energy nonconvexity is the non-monotonicity of the force-elongation relation associated with the global minimum path. In particular, as we see in Fig. 6b, it has a *negative* stiffness at the point where all cross-bridges collectively flip from pre- to post-power-stroke state. The fact that the force can drop down when the system is stretched or jump up when it is shortened is rather unusual from the point of view of a conventional material behavior. Similar mechanical behavior has been recently artificially engineered in *meta-materials* by drawing on the Braess paradox for decentralized globally connected networks [61, 75]. As in our case, the mean-field type coupling in such materials is achieved via parallel connections with multiple shared links. Another biological example of a mechanical system exhibiting negative stiffness is provided by unzipping of RNA and DNA hairpins [67, 76]. In this case the finite temperature is an important part of the physical picture and instead of a localized jump in response to a gradual

loading in a hard device we observe an interval of coherent hopping between two coherent states. In partially folded bio-molecules the long-range interactions originate from the ubiquity of the hairpin structures formed by based-paired segments. Such behavior at finite temperatures, also induced by long-range interactions, has been of course anticipated by the general statistical theory of such systems [62, 77, 78].

B. Soft device

Consider now the HS model loaded in a soft device. Equilibrium states can be found as solutions of the following equations

$$\begin{cases} \left.\dfrac{\partial w}{\partial x_i}\right|_{t,\{x_{j\neq i}\}} = 0 \text{ for all } 1 \leq i \leq N \\ \left.\dfrac{\partial w}{\partial z}\right|_{t,\{x_i\}} = 0 \end{cases}$$

Here t is the control parameter while z and x_i are internal variables. As in the hard device case, the cross-bridges are fully interchangeable and an equilibrium state is fully characterized by the fraction of cross-bridges in the post-power-stroke state p. Each value of the order parameter p defines a branch of local minimizers of the energy (4) parameterized by t, see A. The set of force-elongation relations, characterizing the multitude of these branches, coincide in the cases of soft and hard devices.

At a given value of p, the energy of a metastable state reads

$$\hat{w}(t,p) = -\frac{1}{2}t^2 + pt + \frac{1}{2}p(1-p) + (1-p)v_0. \quad (9)$$

In contrast to the case of a hard device, here there is a nontrivial coupling term $p(1-p)$ describing the energy of mixing. The presence of this term is a signature of a mean-field interaction among individual cross-bridges which, as we have seen, exists in the HS model only in a soft device. The physical mechanism of such interaction can be easily understood. In a soft device the total tension borne by an assembly of cross-bridges has to balance the applied loading t and if one element changes its configuration, its contribution to the common tension changes accordingly and the other elements must adjust to maintain the force balance. Instead, in a hard device, a change of total tension caused by one of the cross-bridges changing its conformational state does not affect other cross-bridges because the common elongation z remains the same. This is the reason why one can expect cooperative behavior in a soft device but not in a hard device.

The tension-elongation relation associated with a set of metastable states sharing the same value of the parameter p can be written in the form

$$\hat{z}(t,p) = -\frac{\partial}{\partial t}\hat{w}(t,p) = t - p.$$

As we have already mentioned, at a given value of p this relation is identical with its counterpart in a hard device, see Eq.7.

The globally stable states can be found by minimizing (9) over p. Since $\partial^2\hat{w}/\partial p^2 = -1$, this function is concave in p, and therefore, as in the case of a hard device, the global minimum is again attained either at $p = 1$ or $p = 0$. The energies of these coherent configurations coincide when $t = t_* = v_0$ and therefore for $t > t_*$ the global minimum is achieved when all cross-bridges are in the pre-power-stroke state ($p = 0$) and for $t < t_*$ when they are all in the post-power-stroke state ($p = 1$).

In Fig. 7(a,b) we illustrate the structure of the energy-tension and the tension-elongation relations corresponding to different values of p for the system with $N = 5$. In Fig. 7(c,d) we zoom into domain near $t = t_*$ and show schematically the response of the system to sudden application of a load increment with an elastic phase ($A \to C_1$) followed by the power-stroke phase $C_1 \to C_2$.

Notice that in contrast to the case of a hard device, the force-elongation relation characterizing the global minimum in a soft device exhibits a plateau signaling a discontinuity in elongation as the cross-bridges switch collectively at $t = t_*$ from pre- to post-power-stroke conformation. This plateau replaces the region of negative stiffness detected in the hard device case and the force-elongation relation becomes monotone.

This difference between the globally stable behaviors in soft and hard devices survives in the limit $N \to \infty$. This suggests that even in the continuum limit the stable "material" responses of our system in hard and soft devices are not equivalent. Such behavior would be completely unexpected from the perspective of classical continuum mechanics, however, it is characteristic of systems with domineering long-range interactions [79]. For instance, similar behavior would be exhibited by the system proposed in [44] as a model of unzipping for biological macromolecules. The actual experiments on RNA discussed in [42] show a slightly different behavior with a tilted plateau because the loading device was of a mixed type.

Another interesting manifestation of the presence of long-range interactions in both soft and hard devices is that a mixture state always has higher energy than at least one of the "pure" states and therefore heterogeneous configurations are energetically suboptimal. Notice, however, that in a hard device the mixture states at the transition point ($z = z_*$) have exactly the same energy as the pure state which suggests the preference of the coherent configurations is "fragile", see Fig. 6(a). Instead, in a soft device there is always a finite energy gap between the pure and mixed states showing that the energetic advantage of the former is robust; see Fig. 12(a). This seemingly trivial observation is behind the fundamental difference in kinetic behavior of muscles in soft and hard devices. It will be further deepened in the study of the regularized HS model in the next section and will resurface again during the analysis of the finite

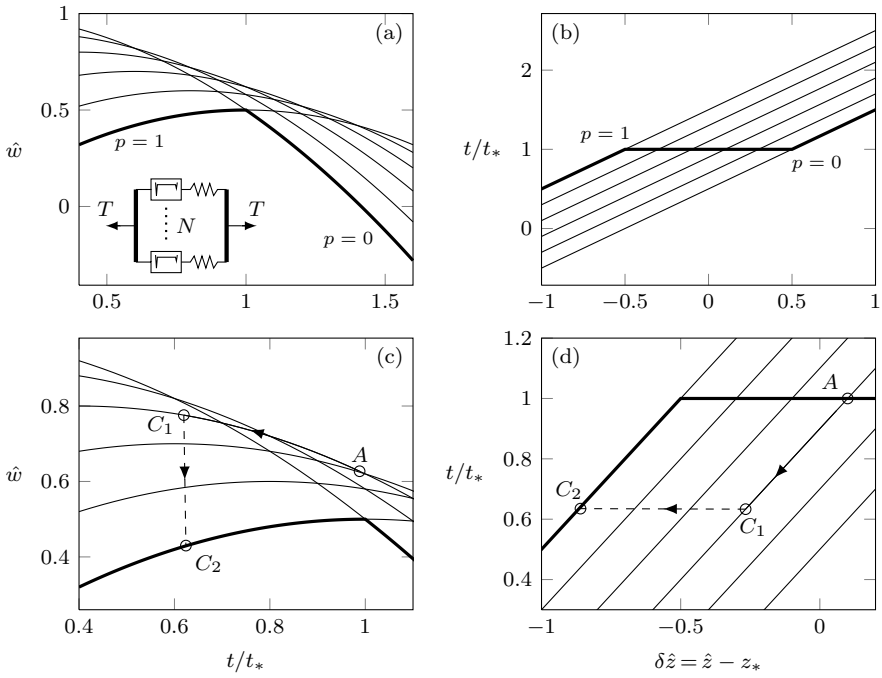

FIG. 7. Mechanical response of the HS model in a soft device. (a) Energy levels of the metastable states ($p = 0, \frac{1}{5}, \ldots, 1$) for different applied forces. (b) corresponding tension-elongation relations. (c)/(d) show details of (a)/(b) with an illustrated response path to fast loading experiment. Thick lines, global minimum corresponding to $p = 0$ / $p = 1$ for $t > t_*$ / $t < t_*$. Parameters are, $v_0 = 1$ and $N = 5$.

temperature effects in paper II [8].

C. Energy barriers

In anticipation of the detailed study of kinetics of the power-stroke in Paper III [9] we can already now pose the question about the size of the energy barrier separating the two conformational states for a parallel bundle of N cross-bridges in soft and hard devices. The corresponding transition state defines the activation energy which play a crucial role in the setting of the rate of the thermally driven transition process.

As we have already seen, in the HS model the transition between the pre- and post-power-stroke states along the global energy minimum path is both abrupt and collective independently of the type of the loading device. This means that the change from a configuration with $p = 0$ to a configuration with $p = 1$ takes place at a single value of the loading parameter and that all cross-bridges undergo the configurational transition simultaneously. However, the implied global minimization does not see the energy barriers separating the corresponding "pure" states and these barriers turn out to be drastically different for our two loading protocols.

We recall that the collective transitions take place at $z = z_*$ in a hard device and $t = t_*$ in a soft device. To access the energy barriers and to find the transition states (saddle points of the energy) we need to study the energy dependence on p at these values of parameters. For general values of the loading parameters this dependence was found to be *linear* in a hard device, indicating that there is no conventional barrier, and *concave* in a soft device which means that there is a barrier. The difference between the corresponding energy landscapes at the threshold values of parameters is illustrated in Fig. 8 (a) for $N = 5$. For the ease of comparison the energy minima are shifted to zero in both loading conditions.

One can see that in a hard device the (excess) energy of all *mixture states* is identically equal to zero which means that the (discrete) activation energy is equal to zero, see the solid line. Instead, in a soft device the (excess) energies of the same configurations are always larger than zero with the transition state corresponding to some $0 < p < 1$, see the dashed line. This observation shows that a switch from pre to post-power-stroke configuration in a soft device carries an energetic cost so the coexisting pure states are robust while in a hard device the transition is cost-free and the coexisting pure states are "fragile". This is in agreement with experimental observations showing much slower power-stroke kinetics in the case of a soft device, see Fig. 3.

To understand the origin of this disparity it is sufficient to consider the minimal HS system with only 2 cross-bridges ($N = 2$); see Fig. 8 (b). Here for simplicity we assumed that $v_0 = 0$ implying $t_* = 0$ and $z_* = -1/2$. The two "pure" configurations are labeled as A ($p = 0$) and C ($p = 1$) at $t = t_* = 0$ and as D ($p = 0$) and B

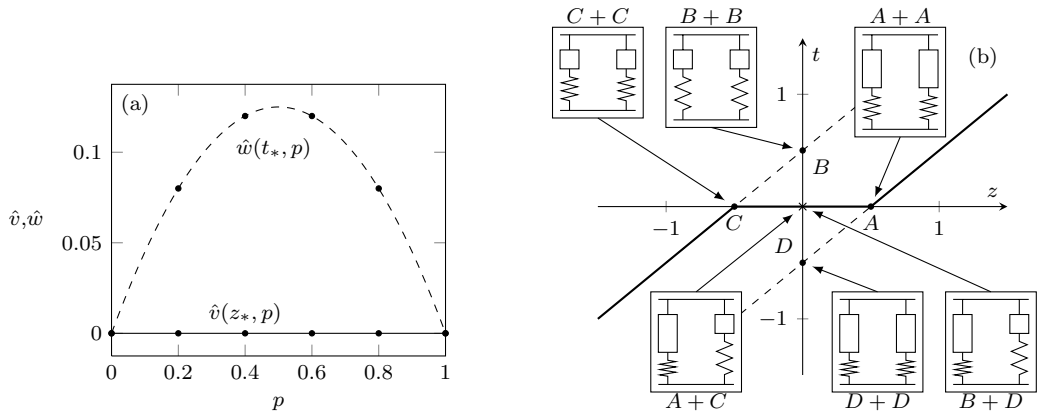

FIG. 8. (a) Energy landscape at the global minimum transition for the HS model. Solid lines, hard device at $z = z_*$; Dashed lines, soft device at $t = t_*$. Dots represent the energy of the different configurations for a system with $N = 5$; lines correspond to the limit $N \to \infty$. Parameters are $v_0 = 1$ and $N = 5$. (b) Representation of the behavior of a system with two cross-bridges with $v_{=0}$ imposing $t_* = 0$ and $z_* = -1/2$, the transition of the global minimum tension-elongation curve (thick) occurring in a stress-free configuration. Dashed lines, metastable states $p = 0$ and $p = 1$. The intermediate stress free configuration is obtained either by mixing the two geometrically compatible states B and D in a hard device which results in a $B + D$ structure without additional internal stress or by mixing the two geometrically incompatible states A and C in a soft device which results in a $A + C$ structure with internal residual stress.

$(p = 1)$ at $z = z_* = -1/2$. In a hard device, where the two elements do not interact, the transition from state D to state B at a given $z = z_*$ goes through the configuration $B+D$ which has the same energy as configurations D and B. Indeed, the cross-bridges in pre- and post-power-stroke states are geometrically perfectly compatible and their mixing requires no additional energy. Instead, in a soft device, where individual elements interact, a transition from state A to state C taking place at a given $t = 0$ requires passing through the transition state $A+C$ which has a nonzero residual stress. The reason is that the individual cross-bridges in this mixture state come with different values of z and therefore the energy of the stressed "mixed" configuration $A + C$ is larger than the energies of the "pure" unstressed states A and C.

To summarize, the barrier in a soft device is higher than in a hard device because because in a soft device a transition is a genuinely cooperative effect requiring essential interaction of individual elements. Instead, in a hard device the conformational change in different cross-bridges takes place independently without any collective interaction. This point will become more clear in the presence of finite temperature (see Paper II, [8]) which breaks the permutational symmetry of the system and spreads the transition along a finite range of loadings. Then the HS model in a hard device does not exhibit a collective phase transition and behaves as paramagnetic system of non-interacting spins. Instead, the behavior of the same system a soft device is ferromagnetic due to the presence of mean-field interactions between individual spins.

It is appropriate to mention here that our description of the barriers in the HS model at finite N is naturally incomplete as in any spin model because of the assumption that the microscopic energy wells are infinitely narrow. This is in fact the reason why the original HS model was not fully mechanical and required a phenomenological closure. The identified deficiency will be addressed in the next section where we show that the microscopic barriers revealed by the regularized model disappear in the continuum limit while the macroscopic barriers, studied in the present section, end up controlling the transition rate between the two homogenous states. We can then conclude that despite its prototypical nature the classical HS model provides the simplest mechanical explanation of the "mysterious" difference between kinetics of the power-stroke in hard and soft devices.

III. THE RHS MODEL

A great advantage of the HS model is that it can capture the main effects associated with fast force recovery, including the non-equivalence of hard and soft loadings, while being analytically transparent. However, such minimal description has its limitations. The main drawback is that the use of hard spins (chemical states), prevents one from recovering the whole energy landscape and modeling dynamics as a continuous stochastic evolution. In particular, as we have seen in the previous section, the HS model remains ambiguous regarding the actual size of the microscopic energy barriers. Another problem is that in the hard device setting the HS model is degenerate because individual cross-bridges do not interact and configurations with different values of the order parameter become equivalent. This suggests infinitely fast kinetics which contradicts observations.

To deal with these problems we regularize the HS

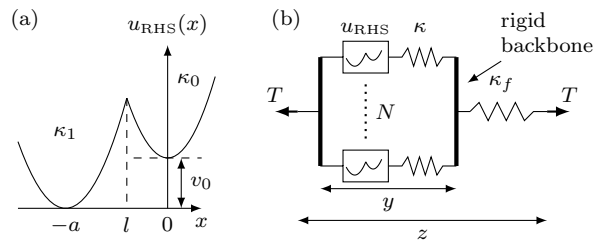

FIG. 9. RHS model of a half-sarcomere. (a) dimensional energy landscape of the head. (b) schematic of a half-sarcomere containing N cross-bridges in a hard device.

model by adding two additional physical mechanisms. The goal is to obtain a minimal model of the next level which is free of the above drawbacks but is still relatively transparent analytically.

First, following [50] we replace hard spins by soft spins, so that x becomes a continuous variable. For simplicity we assume that the corresponding double-well potential can be represented as a minimum of two parabolas (see Fig. 9(a)) and the comparison with the reconstructed potentials for unfolding biological macro-molecules shows that this approximation may be in fact very good [43]. By using non-dimensional variables we can then write

$$u_{\rm RHS}(x) = \begin{cases} \frac{1}{2}\overline{k}_0(x)^2 + \overline{v}_0 & \text{if } x > l \\ \frac{1}{2}\overline{k}_1(x+1)^2 & \text{if } x \le l \end{cases}$$

Here l is the dimensionless position of the energy barrier, $\overline{v}_0$ is the dimensionless energy bias of the post power-stroke state and $\overline{\kappa}_{1,0} = \kappa_{1,0}/\kappa$, are dimensionless elastic moduli of the pre-power-stroke and post-power-stroke states, respectively. In the sequel we drop bars identifying non-dimensional variable for convenience. In the new model the bottoms of the energy wells remain the same as in the HS model but now the barrier separating the two conformational states is well defined, see Fig. 9. It is clear that the bi-quadratic model is too rigid to dissociate the height of the barrier from the transformation strain and the curvatures of the wells so it should be viewed only as a first step.

The mechanical response of a single "soft-spin type" cross-bridge with potential (III) and an attached series spring is governed by the dimensionless energy

$$u_{cb} = u_{\rm RHS}(x) + \frac{1}{2}(y-x)^2$$

where y is the total elongation of a cross-bridge. Equilibrium values of the internal degree of freedom $\overline{x}_1$ and $\overline{x}_0$ are obtained as two solutions of the equation $u'_{\rm RHS}(x) = y - x$, which now depend on the total elongation, see Fig. 10(a). The presence of a finite energy barrier in this modification of the HS model reduces the domain of multi-valuedness of the equilibrium response to a finite interval of y, see Fig 10. Notice the multi-valuedness of the mechanical coupling between the variables x and y and the appearance of the spinodal branch $\overline{x}_*$ that connects the two stable branches $\overline{x}_1(y)$ and $\overline{x}_0(y)$. In the same figure we show the response of this element to a sudden shortening with an elastic unloading in a pre-power-stroke state ($A \to B_1$) followed by the conformational change to a post power-stroke state ($B_1 \to B_2$).

To avoid complete mechanical independence of the cross-bridges in a hard device we should also take into account the finite stiffness of actin and myosin filaments [59, 60]. The induced elastic interaction of individual cross-bridges creates an additional mechanism of self-organization which has been singled out as a possible source of collective oscillations observed in tetanized muscles near the stall force conditions [80, 81]. It is also important that the presence of filament elasticity makes the soft and hard devices less disparate than in the HS model and can create new effects associated with the mixed nature of the loading [58, 71, 82].

Since the detailed account of filament elasticity in the nonlinear mechanical model destroys the transparency of the simplest HS setting we, following [80], use a lump description of filament elasticity by introducing an additional elastic spring with stiffness $\lambda_f = \kappa_f/(N\kappa)$ and the energy

$$u_f(x) = N\frac{\lambda_f}{2}(x)^2.$$

To mimic the mixed loading device we attach this spring in series with our parallel bundle of cross-bridges whose common backbone is now characterized by the internal variable y, see Fig. 9(b). While this approximate way of describing filament elasticity grossly misrepresents short range interactions [58, 83], it allows us to maintain the analytical transparency of the model.

Denoting by z the total elongation, we can write the total energy of the system per cross-bridge in the form

$$v(\boldsymbol{x}, y; z) = \frac{1}{N}\sum_{i=1}^{N}\left[u_{\rm RHS}(x_i) + \frac{1}{2}(y-x_i)^2\right] + \frac{\lambda_f}{2}(z-y)^2. \tag{10}$$

In the hard device case z is the control parameter, x_i are the continuous microscopic internal variables generalizing the spin variables in the HS model and y is a new continuous mesoscopic internal variable. Notice that now even in a hard device the individual cross-bridges are not independent; the implicit mean-field interaction becomes obvious if the variable y is adiabatically eliminated (minimized out). The resulting RHS model (regularized HS model) can then be expected to exhibit in a hard device some features that were characteristic of the behavior of the HS model only in a soft device.

Moreover, the general HS model can be viewed as an asymptotic limit of the RHS model in a hard device. To obtain the hard device case (in HS setting) we need to perform the following double asymtotics: $\overline{\kappa}_{1,0} \to \infty$ and $\lambda_f \to \infty$. The first of these limits ensures that x becomes a spin variable while the second guarantees that $y = z$. To obtain the soft device case we need to consider the

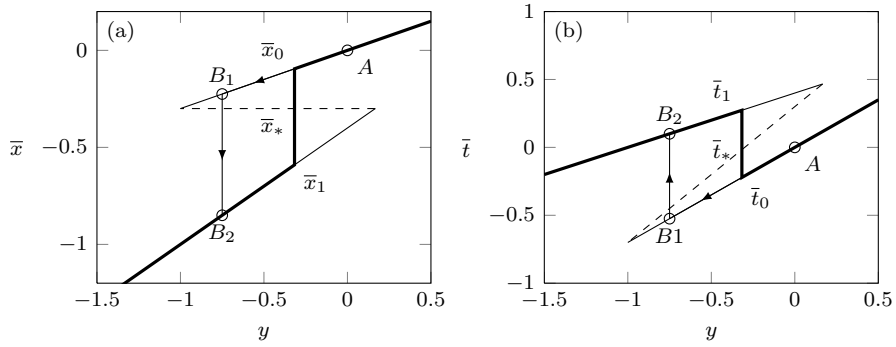

FIG. 10. Properties of a single power-stroke element with the RHS model. (a) equilibrium positions for fixed value of y; (b) equilibrium positions for various y; (c) corresponding tension levels. Solid lines, metastable states; dashed lines, unstable state; bold line, global minimum. Arrows indicate a possible transition between the two metastable states

triple limit: $\overline{\kappa}_{1,0} \to \infty$, $\lambda_f \to 0$ and $z \to \infty$ where the last two limits must be linked in the sense that $\lambda_f z \to t$ ensuring that the force per cross-bridge t remains finite.

In a soft device, the total energy per cross-bridge in the RHS model can be written as

$$w(\boldsymbol{x}, y, z; t) = \frac{1}{N}\sum_{i=1}^{N}\left[u_{\mathrm{RHS}}(x_i) + \frac{1}{2}(y - x_i)^2\right] + \frac{\lambda_f}{2}(z-y)^2 - tz,$$

where $t = T/N$ is again the applied force per cross-bridge. Here the control variable is t while the internal variables are now all three: x_i, y and z. In terms of the structure of internal interactions, this model is not fundamentally different from the HS model in a soft device, however, it contains an important new non-dimensional parameter λ_f allowing one to vary the strength of the interactions between individual cross-bridges.

In the next two subsections, we study more systematically the mechanical response of the RHS model in hard and soft devices.

A. Hard device

To find equilibria of the RHS model in a hard device we need to solve the following system of equations

$$\begin{cases} \left.\dfrac{\partial v}{\partial x_i}\right|_{z,y,\{x_{j\neq i}\}} = 0 \quad \text{for all } 1 \le i \le N & \text{(11a)} \\ \left.\dfrac{\partial v}{\partial y}\right|_{z,\{x_i\}} = 0 & \text{(11b)} \end{cases}$$

Equations Eq.11a have up to 3 solutions that can be parameterized by y,

$$\begin{cases} \overline{x}_1(y) = (1-\lambda_1)(y) - \lambda_1, & \text{if } x_1 < l \\ \overline{x}_0(y) = (1-\lambda_0)(y), & \text{if } x_0 > l \\ \overline{x}_* = l. \end{cases} \qquad (12)$$

Here we have redefined our dimensionless parameters

$$\lambda_0 = \frac{\kappa_0}{1+\kappa_0}, \quad \lambda_1 = \frac{\kappa_1}{1+\kappa_1}.$$

By using Eq.11b we can explicitly express the mesoscopic variable y through the microscopic variables x_i,

$$\overline{y}(\boldsymbol{x}; z) = \frac{1}{1+\lambda_f}\left(\lambda_f z + \frac{1}{N}\sum_{i=1}^{N} x_i\right). \qquad (13)$$

Because of the permutational invariance the equilibrium solution of (11) is fully characterized by $p = \frac{1}{N}\sum_{i=1}^{N}\alpha_i$, the fraction of cross-bridges in the post-power-stroke conformation, an $r = \frac{1}{N}\sum_{i=1}^{N}(1-\alpha_i)$, the fraction of cross-bridges in the pre-power-stroke conformation. Here we defined an auxiliary spin variable

$$\alpha_i = \begin{cases} 1 & \text{if } x_i = \overline{x}_1 \\ 0 & \text{if } x_0 = \overline{x}_0 \end{cases}$$

The fraction of cross-bridges at the "spinodal" point $\overline{x}_*$ can be now written as $q = 1 - p - r$.

By using (13), we can eliminate the variable y and obtain an explicit representation of the microconfiguration in terms of (p, q, r)

$$\hat{y}(z, p, q, r) = \frac{\lambda_f}{\lambda_f + \Lambda(p,q,r)}\left(z - \frac{p\lambda_1 - ql}{\lambda_f}\right) \qquad (14)$$

$$\hat{x}_1(z, p, q, r) = \frac{1-\lambda_1}{\lambda_f + \Lambda(p,q,r)}(\lambda_f z - p\lambda_1 + ql) - \lambda_1 \qquad (15)$$

$$\hat{x}_0(z, p, q, r) = \frac{1-\lambda_0}{\lambda_f + \Lambda(p,q,r)}(\lambda_f z - p\lambda_1 + ql) \qquad (16)$$

Here $\Lambda(p, q, r) = p\lambda_1 + q + r\lambda_0$, represents the equivalent stiffness of the parallel bundle of cross-bridges in a mixed configuration parameterized by (p, q, r).

The energies of the equilibrium configurations can be

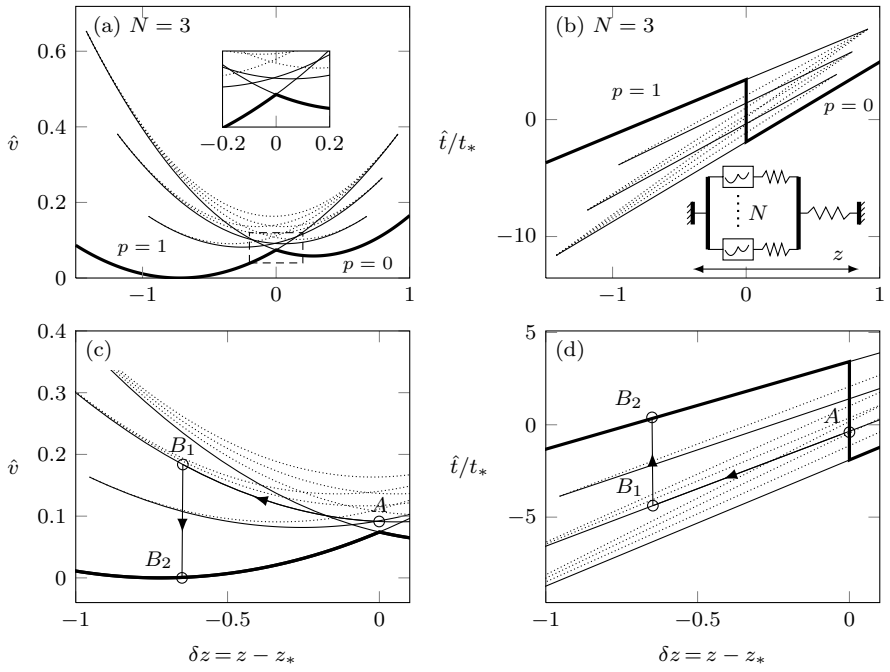

FIG. 11. Mechanical response of the RHS model in a hard device. (a) Energy levels of all the (p, q, r) configurations for the case $N = 3$ for different applied elongations. The insert in (a) shows the details in the dashed square. (b) corresponding tension-elongation relations. Solid lines, metastable states with $p = 0, 1/3, 2/3, 1$ and $r = 1 - p$, $q = 0$; dotted lines, unstable state with $q \neq 0$; thick lines, global minimum corresponding to $p = 0$, $r = 1$, for $z > z_*$, and to $p = 1$, $r = 0$, for / $z < z_*$. (c,d) blow-up of (a,b) illustrating the response of the system to abrupt shortening with an elastic unloading ($A \to B_1$) followed by a massive conformational change in isometric conditions ($B_1 \to B_2$). Parameters are, $\lambda_1 = 0.4$, $\lambda_0 = 0.7$, $l = -0.3$, $\lambda_f = 1$ and $N = 3$.

now computed explicitly. For a given (p, q, r) we obtain

$$\hat{v}(z,p,q,r) = \frac{1}{2}\left[\frac{\lambda_f\left[p\lambda_1(z+1)^2 + q(z-l)^2 + r\lambda_0 z^2\right]}{\lambda_f + \Lambda(p,q,r)} + \frac{p\lambda_1\left[r\lambda_0 + q(1+2l)\right] - ql^2(q+\lambda_f)}{\lambda_f + \Lambda(p,q,r)} + \frac{ql^2}{1-\lambda_0} + 2(q+r)v_0\right]. \quad (17)$$

The corresponding tension-elongation curves can be written as

$$\hat{t}\,(z,p,q,r) = \frac{\partial}{\partial z}\hat{v}(z,p,q,r) = \frac{\lambda_f\Lambda(p,q,r)}{\lambda_f + \Lambda(p,q,r)}\left(z + \frac{p\lambda_1 - ql}{\Lambda(p,q,r)}\right).$$

Each discrete set of parameters (p, q, r) defines an equilibrium branch which extends between the two limits $[z_{\rm inf}, z_{\rm sup}]$ induced by the inequalities $\hat{x}_1 < l$ and $\hat{x}_0 > l$. These limits can be computed explicitly

$$z_{\rm inf}(p,q,r) = \frac{l(\lambda_f + \Lambda(p,q,r)) + (1-\lambda_0)(p\lambda_1 - ql)}{\lambda_f(1-\lambda_0)},$$

$$z_{\rm sup}(p,q,r) = \frac{(l+\lambda_1)\big(\lambda_f + \Lambda(p,q,r)\big)}{\lambda_f(1-\lambda_1)} + \frac{(1-\lambda_1)(p\lambda_1 - ql)}{\lambda_f(1-\lambda_1)}.$$

The compactness of the equilibrium branches associated with the finiteness of the energy barriers is a major difference between the RHS model and the HS model where each equilibrium branch could be extended for all values of the loading parameter. Notice also that in the case ($\lambda_f = \infty$) studied in [50] when the filament elasticity is absent and the cross-bridges do not interact, these boundaries become independent of the configuration: $z_{\rm inf} = l/(1-\lambda_0)$ and $z_{\rm sup} = (l+\lambda_1)/(1-\lambda_1)$.

To identify local minima (metastable states) among the equilibrium states we need to compute the Hessian of the function $v(x_i, y)$. The analysis presented in A shows that all equilibria are stable except for the ones with $q \neq 0$ that are unstable. Therefore, as in the HS model, the metastable configurations can be parameterized by a single parameter p.

The obtained results are illustrated in Fig. 11(a,b) where we show the complete set of equilibria for the RHS

model in a hard device with $N = 3$. The metastable branches are indicated by solid lines and the unstable ones - by dotted lines. In Fig 11(c,d) we show a blow up illustrating the response of the system to abrupt shortening with an elastic unloading ($A \to B_1$) followed by a massive conformational change in isometric conditions ($B_1 \to B_2$).

Notice that the global minimum of the energy, shown by a bold line, is again achieved exclusively on homogeneous configurations configurations $(1, 0, 0)$ and $(0, 0, 1)$. To show this analytically, we assume that $r = 0, q = 1-p$ and compute the second derivatives of v in (17) while interpreting p as a continuous variable

$$\frac{\partial^2}{\partial p^2}\hat{v}\left(z,p\right) = -\frac{1}{2}\frac{\left[\lambda_f\lambda_1\left(z+1\right)+\lambda_0\left(\lambda_1-z\lambda_f\right)\right]^2}{\left[p\lambda_1+\left(1-p\right)\lambda_0+\lambda_f\right]^3} \leq 0. \tag{18}$$

The obtained inequality shows that the energy is concave, which means that the global minimum is reached on fully synchronized configurations. The switch between the two homogeneous states takes place at the $z = z_*$ which solves $\hat{v}(z, 0, 0, 1) = \hat{v}(z, 1, 0, 0)$. While the global minimum path in the RHS model has the same structure as in the HS model, we see that in the transition point $z = z_*$ the energies of the mixture states are strictly higher than the energies of the coexisting pure states, see the insert in Fig. 11. This shows that in RHS the coherent states in a hard device are no longer "fragile" and the synchronization is robust. This is of course an effect of the mean-field interaction between individual cross-bridges which is induced by the account of filament elasticity and which disappears in the HS limit $\lambda_f \to \infty$.

The computed force-elongation relations are shown in Fig. 11(b). The basic structure of the global minimum path is the same as in the HS model with a finite jump at $z = z_*$. The difference is that now similar jump can occurs if the system occupying one of the mixed metastable configurations is driven beyond the limit of stability of the corresponding inhomogeneous state. Instead, in the HS model such stability limits are absent and the metastable branches extend to infinity.

One can see, however, that the singular meta-material behavior exhibited by the HS model was not regularized in the RHS model where the stiffness corresponding to the globally stable response is still equal to $-\infty$ at a single point and the picture remains the same in the limit $N \to \infty$. To account appropriately for the the capacity of the system to develop a gradual "tension" increment under shortening and a gradual "compression" increment under lengthening, the lump description of filament elasticity is not sufficient and a process of the wave type *propagation* of the power-stroke transition along the filament must be taken into consideration.

B. Soft device

As we have already mentioned, the behavior of the RHS model in a soft device is not fundamentally different from the behavior of the HS model except for the finiteness of the equilibrium branches. Both models account adequately for the mean-field interaction among the cross-bridges and describe similarly robust cooperative effects.

More specifically, to find equilibrium states in the RHS model loaded in a soft device we need to solve the following system

$$\begin{cases} \left.\dfrac{\partial w}{\partial x_i}\right|_{t,z,y,\{x_{j\neq i}\}} = 0 \text{ for all } 1 \leq i \leq N \\ \left.\dfrac{\partial w}{\partial y}\right|_{t,z,\{x_i\}} = 0 \\ \left.\dfrac{\partial w}{\partial z}\right|_{t,y,\{x_i\}} = 0. \end{cases}$$

As in the hard device case, each cross-bridge can be in three states and the equilibrium branches can be parameterized by the triplet (p, q, r)

$$\begin{aligned} \hat{y}(t,p,q,r) &= \frac{1}{\Lambda(p,q,r)}t - \frac{p\lambda_1 - ql}{\Lambda(p,q,r)} \\ \hat{x}_1(t,p,q,r) &= \frac{(1-\lambda_1)}{\Lambda(p,q,r)}(t - p\lambda_1 + ql) - \lambda_1, \\ \hat{x}_0(t,p,q,r) &= \frac{(1-\lambda_0)}{\Lambda(p,q,r)}(t - p\lambda_1 + ql). \end{aligned}$$

The energy of a configuration (p, q, r) can be again computed explicitly

$$\hat{w}(t,p,q,r) = -\frac{1}{2}\left[\frac{1}{\Lambda(p,q,r)}(t-p\lambda_1+ql)^2 + \frac{t^2}{\lambda_f} - 2(q+r)v_0 - q\frac{l^2}{1-\lambda_0} - p\lambda_1\right].$$

The corresponding tension-elongation relations read

$$\begin{aligned} \hat{z}\left(t,p,q,r\right) &= -\frac{\partial}{\partial t}\hat{w}(t,p,q,r) \\ &= \left(\frac{1}{\lambda_f} + \frac{1}{\Lambda(p,q,r)}\right)t - \frac{p\lambda_1 - ql}{\Lambda(p,q,r)}. \end{aligned}$$

Finally, we can write the expressions for the lower and upper boundaries of a branch labeled by (p, q, r)

$$\begin{aligned} t_{\sup}(p,q,r) &= \frac{l+\lambda_1}{1-\lambda_1}\Lambda(p,q,r) + p\lambda_1 - ql, \\ t_{\inf}(p,q,r) &= \frac{l}{1-\lambda_0}\Lambda(p,q,r) + p\lambda_1 - ql. \end{aligned}$$

The stability analysis shows again – see A– that configurations with $q \neq 0$ are unstable and therefore all

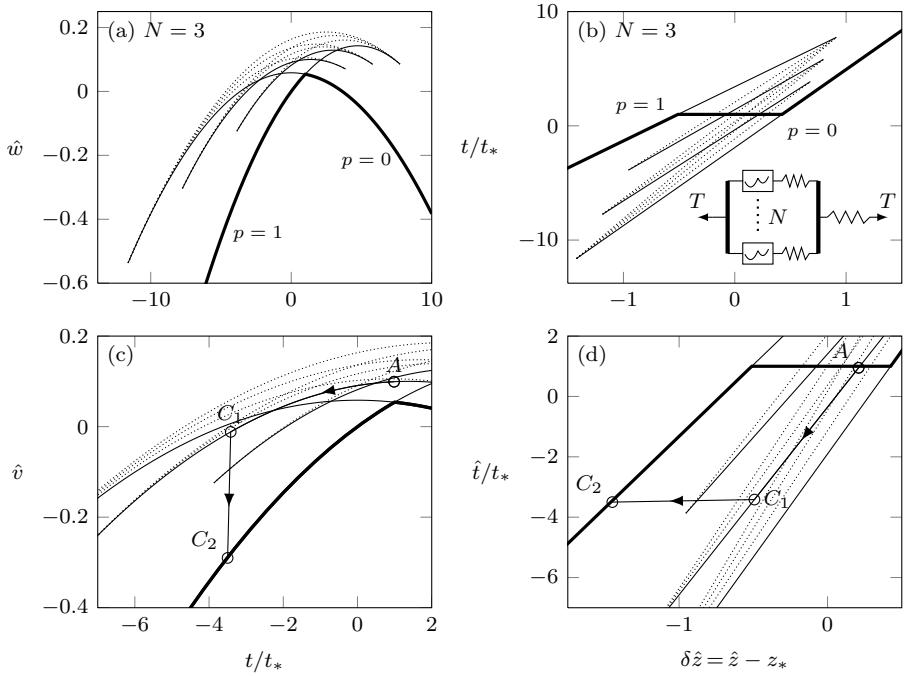

FIG. 12. Mechanical response of the RHS model in a soft device. (a) Energy levels of all the (p, q, r) configurations for the case $N = 3$ for different applied tensions. (b) corresponding tension-elongation relations. Solid lines, metastable states with $p = 0, 1/3, 2/3, 1$ and $r = 1 - p$, $q = 0$; dotted lines, unstable state with $r \neq 0$; thick lines, global minimum corresponding to $p = 0$, $r = 1$ for $t > t_*$ and to $p = 1$, $r = 0$, for / $t < t_*$. (c,d) blow-up of (a,b) illustrating the response of the system to abrupt shortening with an elastic unloading ($A \to B_1$) followed by a massive conformational change in isometric conditions ($B_1 \to B_2$). Parameters are as in Fig. 11.

metastable states can be parameterized by a single parameter p. Since

$$\frac{\partial^2}{\partial p^2}\hat{w}\left(t,p\right) = -\left[\frac{\left(\lambda_1-\lambda_0\right)^2\left(t-p\lambda_1\right)^2}{\left(p\lambda_1+\left(1-p\right)\lambda_0\right)^3} + \frac{\lambda_1^2}{p\lambda_1+\left(1-p\right)\lambda_0}\right] \leq 0,$$

the global minimum is again attained either at $p = 1$ or $p = 0$ and these pure states are robust. The switch between them, signaling a collective power-stroke, takes place at $t = t_*$ satisfying $\hat{w}(t, 1, 0, 0) = \hat{w}(t, 0, 0, 1)$.

The equilibrium response of the RHS model in a soft device is illustrated in Fig. 12 where we show the energies of all equilibrium branches and the corresponding tension-elongation curves; metastable branches are shown by solid lines, unstable branches by dotted lines and the global minimum path is presented by a bold line. The individual $t(\delta z)$ curves for metastable equilibria are the same in soft and hard devices and the difference between the two protocols can be again seen only if we consider the global minimum path. As in the case of the HS model, here we do not observe any jumps in stress that can be interpreted as a negative stiffness behavior. Instead, the globally stable response contains an extended plateau at $t = t_*$, see Fig. 12b.

Although we illustrated the obtained explicit formulas for the case $N = 3$, it is clear that the constitutive behavior of the system remains quantitatively the same in the continuum limit $N \to \infty$. While the distribution of branches in the metastability domain becomes dense, the global minimum force-elongation relation remains monotone. This suggests that in hard and soft device loadings the RHS model generates fundamentally different globally stable responses and that this difference persists even in the continuum/thermodynamic limit. We reiterate that this nontrivial effect of the domineering long-range interactions can be already captured at the basic level by the classical HS model.

C. Energy barriers

We now turn to the analysis of energy barriers ultimately controlling the kinetics of fast force recovery. We recall that in the HS model individual microscopic spin states were not connected and the transitions between them had to be interpreted as jumps. Instead, in the RHS model the energy landscape is continuous and the barriers can be characterized exhaustively.

Consider first the case of a hard device and assume that at a chosen value of z we have two homogeneous equilibria with $p = 0$ and $p = 1$ with one of them being

globally stable. The energy minimizing "reaction path" connecting these homogeneous states goes through a set of inhomogeneous metastable states with $0 < p < 1$. The energies of these states can be obtained by putting $q = 0, r = 1 - p$ in (17)

$$\hat{v}(z,p) = \frac{1}{2}\left[\frac{\lambda_f\big(p\lambda_1(z+1)^2 + (1-p)\lambda_0 z^2\big)}{\lambda_f + \Lambda[p,0,(1-p)]} + \frac{p\lambda_1(1-p)\lambda_0}{\lambda_f + \Lambda[p,0,(1-p)]} + 2(1-p)v_0\right].$$

We know that for $\lambda_f < \infty$ the function $\hat{v}(z,p)$ is concave in p, see Eq. 18. If p was a continuous variable the maximum of this function at $0 < p < 1$ would characterize the "transition state". However, at finite N the variable p is discrete and to characterize the transition state we need to described the microscopic barriers separating configurations with different values of p. These barriers, associated with the conformational changes in individual cross-bridges, were essentially infinite in the HS model.

The fine structure of the energy barriers can be reconstructed in the RHS model. To this end, consider a metastable configuration with N_0 cross-bridges in the pre power-stroke state and $N_1 = N - N_0$ cross-bridges in the post-power-stroke state. We have shown before that this configuration is fully characterized by the parameter $p = N_1/N$. Suppose that now that a single cross-bridge switches from pre to post-power-stroke state. To find the barrier which the system has to overcome, we need to choose a microscopic "reaction path" separating the initial configuration characterized by p and the final configuration characterized by $p + 1/N$. It is natural to assume that the "reaction coordinate" is the strain x_i in the cross-bridge with index i undergoing the conformational change. Due to permutational invariance (mean-field type interaction) the transforming element may be chosen arbitrarily among the N_0 elements that are initially in the pre power-stroke state and without loss of generality we assume that $i = N$. To find the energy variation along this reaction path we need to minimize out the rest of the internal variables $x_1, \ldots, x_{N-1}, y$. We obtain

$$\begin{aligned}\overline{v}(p,z,x_N) = {} & p\frac{\lambda_1}{2}\left[\overline{y}(p,z) + \epsilon(p,x_N) + 1\right]^2 \\ & + (1-p)\left(\frac{\lambda_0}{2}\left[\overline{y}(p,z) + \epsilon(p,x_N)\right]^2 + v_0\right) \\ & + \frac{1}{N}\left(u_{\rm RHS}(x) + \frac{1}{2}\left[\overline{y}(p,z) + \epsilon(p,x_N) - x_N\right]^2\right) \\ & + \frac{\lambda_f}{2}\left[z - \overline{y}(p,z) - \epsilon(p,x_N)\right]^2 \quad (19)\end{aligned}$$

where

$$\overline{y}(p,z) = \frac{1}{\lambda_f + 1/N + p\lambda_1 + (1-p)\lambda_0}\left(\lambda_f z - p\lambda_1\right)$$

$$\epsilon(p,x_N) = \frac{x_N}{N\left(\lambda_f + 1/N + p\lambda_1 + (1-p)\lambda_0\right)}.$$

For convenience we map the reaction coordinate to the interval $[p, p + 1/N]$ by replacing x_N with a stretched variable ξ defined by

$$\xi = p + \frac{1}{N}\frac{x_N - \hat{x}_0(p,z)}{\hat{x}_1(p+1/N,z) - \hat{x}_0(p,z)}.$$

where $\hat{x}_0$ and $\hat{x}_1$ are the locations of the bottoms of the energy wells defined by Eqs.15 and 16. The values $\xi = p$ and $\xi = p+1/N$ are associated with the metastable states $\hat{v}(p, q = 0, r)$ and $\hat{v}(p+1/N, q = 0, r-1/N)$, respectively, see Eq. 6. At $\xi = p + (1/N)(l - \hat{x}_0)/(\hat{x}_1 - \hat{x}_0)$, we have $x_N = l$ and the energy has a local maximum, namely $\hat{v}(p, q = 1/N, r - 1/N)$, corresponding the the configuration with exactly one spring in the spinodal state. These states belong to the unstable equilibrium branches characterized by $q > 0$ and shown in Fig. 11 by dotted lines. It is clear that now the same variable ξ can be used to describe transitions between successive pairs of neighboring metastable states at different values of p.

To facilitate comparison with the HS model we shall again limit our attention to the barriers associated with the transition between the two globally stable coherent states taking place at $z = z_*$. The combined energy landscape $\overline{v}(\xi)$ at $z = z_*$ is shown in Fig. 13(a) where we compare two cases, $N = 5$ and $N \to \infty$. At finite N we observe a *macroscopic barrier*, not captured by the HS model, with a superimposed set of *microscopic barriers* representing the "lattice pinning". These microscopic barriers are due to the discreetness of the problem and they disappear in the continuum/thermodynamic limit $N = \infty$ where $\xi \to p$; see the dashed line.

To summarize, we identified here two new effects vis-à-vis the HS model. First, in a hard device at $z = z_*$ the HS models predicted that the macroscopic barrier is absent. The presence of a nonzero macroscopic barrier in the RHS model is due to the account of the filament elasticity which brings a mean-field coupling which robustly favors synchronized states. The second effect is related to the ruggedness of the energy landscape at the microscale which was not resolved at all in the HS model. This fine structure of the energy has nothing to do with filament elasticity and is fully determined by the bi-quadratic potential describing the power-stroke in a single myosin head. One can see that both new elements distinguishing the RHS model from the HS model are essential.

Similar structure of the energy along the reaction path connecting two coherent states can be reconstructed for the RHS system in a soft device. In this case the partially

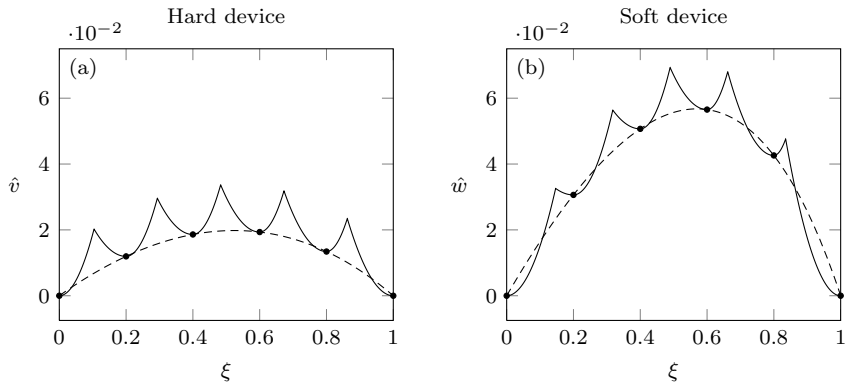

FIG. 13. Energy landscape at the global minimum transition for the RHS model with $N = 5$. (a) hard device; (b), soft device. Solid lines, successive barriers obtained from Eqs. 19 (a) and 20 (b); Dashed lines, continuum limit, $N \to \infty$. Energy minima are arbitrarily set to 0 for comparison. Here, $\lambda_f = 1$ and other parameters are as in Fig. 11.

equilibrated energy at fixed t, p and x_N has the form

$$\begin{aligned}\overline{w}(p,t,x_N) &= p\frac{\lambda_1}{2}\left[\overline{y}(p,t)+\epsilon(p,x_N)+1\right]^2 \\ &+ (1-p)\left[\frac{\lambda_0}{2}\left[\overline{y}(p,t)+\epsilon(p,x_N)\right]^2+v_0\right] \\ &+ \frac{1}{N}\left(u_{\rm RHS}(x_N)+\frac{1}{2}\left[\overline{y}(p,t)+\epsilon(p,x_N)-x_N\right]^2\right) \\ &+ \frac{\lambda_f}{2}\left[\overline{z}(p,t)-\overline{y}(p,t)-\epsilon(p,x_N)\right]^2 - t\overline{z}(p,t) \quad (20)\end{aligned}$$

where

$$\begin{aligned}\overline{y}(p,t) &= \frac{1}{1/N+p\lambda_1+(1-p)\lambda_0}\left(t-p\lambda_1\right) \\ \overline{z}(p,t) &= \overline{y}(p,t)+t/\lambda_f \\ \epsilon(p,x_N) &= \frac{x}{N\left(1/N+p\lambda_1+(1-p)\lambda_0\right)}.\end{aligned}$$

By using this expression for the energy it is now easy to reconstruct the energy landscape $\overline{w}(\xi)$, where the variable ξ has the same meaning as in a hard device.

The fine structure of the typical energy landscape is illustrated in Fig. 13(b) for $t = t_*$. At finite N we see again the same two-scale structure, however, the overall barrier is markedly higher in a soft than in a hard device. The macroscopic barrier can be adequately captured by studying the case $N = \infty$ while the recovery of the microscopic structure of the energy landscape requires the account of the discreetness.

To see the relation between the HS model and the RHS models at finite N more clearly we present in Fig. 14(a) the dependence of the energy landscape for the system in a hard device at the transition point $z = z_*$ on the parameter λ_f characterizing filament elasticity. To simplify the comparison we adjusted the parameter $z = z_*$ at each value of λ_f so that the coherent states with $p = 0$ and $p = 1$ have the energy equal to zero. As we know, the RHS model converges to the HS model as $\lambda_f \to \infty$ and we see in Fig. 14(a) that the "macroscopic barrier" disappears in this limit. The microscopic barriers remain and that is what distinguishes the model proposed in [50] from the HS model. Of course, in the continuum limit $N \to \infty$ illustrated in Fig. 14(b) we lose the microscopic barriers and recover the interpolated predictions of the classical HS model.

Another interesting case shown in the same figure is the limit $\lambda_f \to 0$ when $z_* \to \infty$. In this case we recover in the hard device setting the predictions of the system loaded in a soft device with $t \to t_*$. Indeed, one can see that the energy landscape at $N = 5$ corresponding to $\lambda_f = 0$ in Fig. 14 is exactly the same as the energy landscape shown in Fig. 13(b). Once again, in the continuum limit $N \to \infty$ the microscopic barriers disappear and we recover the basic picture predicted by the HS model.

The analysis of the structure of the energy barriers along a particular path in the configurational space reveals the global complexity of the underlying energy landscape. In the language of chemo-mechanical models the individual local minima of this landscape, representing various metastable configurations, can be interpreted as distinct discrete *chemical states* and the kinetics of unfolding can modeled as set of jump transitions between these states. However, the exponentially growth of the number of such states in the thermodynamic limit suggests that a description in terms of individual energy wells is hardly productive. Instead, the description in terms of macro-wells, corresponding to *synchronized configurations*, appears to be more appropriate and can lead to an adequate quasi-chemical representation of the loading-induced folding process. In a larger scale depiction of muscle machinery, incorporating several layers of structure, the coherent energy wells, describing synchronized states at particular scales, are most probably hierarchically structured as in protein-folding problem and the description of such mechanical system in terms of chemical pathways presents a formidable challenge.

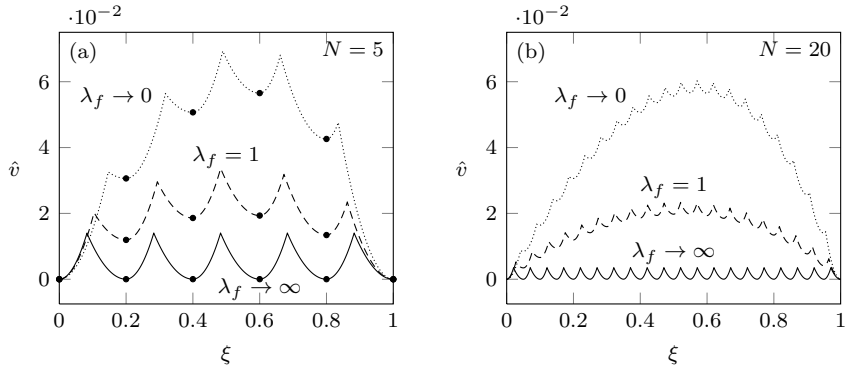

FIG. 14. Energy landscape at the global minimum transition for the RHS model in a hard device at different values of the coupling parameter λ_f. (a) with $N = 5$; (b), with $N = 20$. Solid lines, hard device with $\lambda_f \to \infty$; dashed lines, hard device with $\lambda_f = 1$; dotted lines, soft device limit as the hard device case where $\lambda_f \to 0$. Energy minima are arbitrarily set to 0 for comparison. Other parameters are as in Fig. 11.

IV. DISCUSSION

In contrast to inert matter, distributed biological systems are characterized by structurally complex network architecture with domineering long-range interactions. This leads, even in the absence of ATP driving, to a highly unusual passive mechanical behavior in both statics and dynamics. In this paper we identified the simplest system of this type representing a muscle half-sarcomere and systematically studied its peculiar response to fast loading when the ATP activity can be neglected. We showed that the implied anomalies of the mechanical behavior are indeed due to the dominance of long-range interactions and that they can be adequately represented already at zero temperature by a simple prototypical model.

Our starting point was the classical HS model which deals with a parallel bundle of bi-stable elements, see [17]. In this model the two states, describing pre- and post-power-stroke configurations, are represented as hard spin states. Over the years the HS model was studied exclusively in the hard device loading conditions which concealed the important role of cooperative effects. The original HS paper also offered an insight regarding the possibility of stable negative stiffness, which is now interpreted as a meta-material behavior, however, this subtle message remained largely unnoticed or undermined.

Our mechanical reevaluation of the HS model showed that it behaves superficially similarly in soft and hard devices exhibiting always highly cooperative globally stable behavior with all cross-bridges striking at the same moment. However, our analysis also showed that in a hard device the cooperative behavior is "fragile" because the macroscopic energy wells, describing coherent states, are not separated by any barrier. As a result at any nonzero temperature the system can be expected to lose the coherency and indeed, as Huxley and Simmons showed in their classical paper, the finite temperature behavior in a hard device is completely de-synchronized. Our contribution to this problem is the demonstration that the same HS model would behave rather differently in a soft device. In particular, we showed that in a soft device the macroscopic wells of HS model become robust in the sense that the separating barrier is now finite. The cooperative behavior in a soft device setting can then be expected to survive at least for small temperatures.

In [50] the hard spins constituting the essence of the HS approach were replaced by soft spins. This allowed the authors to achieve better quantitative agreement with experiment, in particular, to explain the stress dependence of the power-stroke. Such augmentation has also led to the specification of the energy barriers between microscopic configurations that remained ambiguous in the original HS setting. In the present paper, we made the next step and developed a regularized RHS model containing a crucial new element. By introducing the simplest lump description of filament elasticity we relaxed the hard device constraint of the HS model opening the possibility for individual cross-bridges to interact and to self-organize into macroscopically coherent states. We showed that a low propensity towards the formation of such highly synchronized states is the main factor behind the anomalously fast force recovery in a hard devices comparing to the same experiments in a soft device. Drastically different kinetic responses in these two loading conditions have been previously experimentally identified but remained unexplained.

As a result of our regularization of the HS model, we were able to trace the gradual enhancement of the collective effects as the system is progressively converted from hard to soft device. More specifically we have shown that in the presence of mean-field interactions induced by the coupling through a common backbone, the transition between the two conformations of the attached cross-bridges cannot be perceived as a sequence of consecutive switching events because of the high energy cost involved in such transitions. Instead, the identified optimal "reaction path" is associated with a collective power-stroke.

This observation explains the accelerated kinetics in the case of a hard device where the long-range interactions are much weaker than in a soft device.

More generally, we observed that the mechanical behavior of HS and RHS models is different in soft and hard device and showed that this disparity persists even in the continuum limit. Such systematic non-equivalence of the loading "ensembles" is also a manifestation of long-range interactions leading to non-additivity of the total energy of the system [62, 84]. In such systems where each element is linked with almost equal strength with all other elements, parts interact in a non-simple way and the whole is not a sum of the parts. Our paper presents an interesting example of such behavior in the realm of purely mechanical systems where the continuum limit was traditionally perceived as ensemble independent [85].

An interesting feature of the proposed model is the possibility of negative stiffness. The mechanical intuition, based on the study of materials with short range interactions, suggests that in a stable continuum system the relaxed energy must must be convex (at least in 1D) and that the corresponding stiffness must be positive. This conclusion is based on the idea that the energy can be always convexified by mixing states with different energies. As our paper shows, in systems with long-range interactions mixing does not necessarily lower the energy and the highly coherent "pure" states may always have the lowest energy. Although the possibility of sign reversal of equilibrium susceptibilities in systems with long-range interactions, for instance, in self-gravitating systems [62], has been previously known, the biological application of this idea appears to be new.

The RHS model is further developed in the companion Paper II [8], where we study the effects of finite temperature and replace the energy minimization by the computation of statistical sums. It is not surprising that due to the minimal nature of our model (piece-wise quadratic potential, simplified account of filament elasticity, etc.) a transparent semi-analytical description is available also at finite temperatures. An important new feature of the thermo-mechanical model is the appearance of a critical point separating the correlated behavior at low temperatures from the uncorrelated behavior at high temperatures. It is quite remarkable that actual skeletal muscles appear to be functioning very close to this critical point. To corroborate this statement we developed in the third paper of this series, Paper III [9], a consistent method of extracting realistic values of parameters from experimental data. Based on these data we developed in Paper III a comprehensive thermo-mechanical model of muscle behavior showing that the RHS model can match quantitatively both equilibrium and kinetic observations.

The conclusions drawn from the analysis of our prototypical model can be used in the study various other systems with multi-stable or breakable elements interacting through a network of effective backbones that are able to transmit long-range interactions. Our study emphasizes the fundamental difference in the response of such system under isotonic or isometric loadings and explains the origin of their cooperative behavior.

An important example of such systems is provided by adhesive clusters, where the long-range mechanical coupling of individual binders through quasi-rigid pads also leads to synchronization [63, 86–88]. In this framework an idea of a prototypical "parallel cluster" has emerged which is quite similar to our model of a half-sarcomere [53]. The main difference is that our approach is purely mechanical implying continuous stochastic dynamics, while the evolution in the models of adhesive binders is discrete and the long-range interaction is introduced through the force dependence of kinetic constants. Therefore, these models are closer to the HS model than to RHS model. Similar ideas of force dependent chemistry were also applied to muscle contraction, however, the resultant cooperative behavior was previously thought as inseparable from the ATP activity breaking the detailed balance [40, 80, 89].

Other examples of synchronized folding-unfolding phenomena can be found in the studies of mechanically loaded biological macromolecules, where the hairpins and partially folded intermediates are usually supported by effective backbones. It is then not surprising that in these systems the cooperative hopping (or flip-flopping) between unfolded and refolded states was found to be ubiquitous [42, 44, 67, 76]. A related effect is that the force extension curves for folding and unfolding macromolecules, obtained from single molecule force spectroscopy measurements, exhibit characteristic plateaus/jumps. The individual steps on these curves are usually associated with synchronized unfolding at a particular scale and the corresponding discrete force/elongation increments are sometimes interpreted as "fracture" avalanches [90].

The importance of the topology of interconnections among the bonds has been also emphasized in the studies of protein folding where the link between the cooperativity of unfolding and the dominance of parallel bonding was noticed [54]. It is also known that proteins and nucleic acids behave differently in isometric and isotonic conditions and that these mechanical systems can exhibit negative stiffness [55, 69, 91]. However, various observations of this type have not been previously linked together. Therefore, by emphasizing the crucial role of the force transmitting backbones in all these observations, our study bridges an important gap and provides a prototypical description of this class of phenomena in a framework of a simple paradigmatic system. Moreover, the transparent mechanical nature of our model suggests an explicit path towards designing bio-mimetic materials and molecular nano-machines whose functioning depends essentially on long-range feedback between multi-stable units [92].

Acknowledgements. The authors are grateful to P. Recho, R. Sheshka and V. Lombardi for helpful discussions. M.C. also thanks Ecole Polytechnique for financial

support through the Monge Doctoral Fellowship.

Appendix A

The analysis of stability is similar in the HS and RHS models. A small technical complication is that in both cases the bistable potentials $u_{\rm HS}$ and $u_{\rm RHS}$ are both singular. Thus, in the HS model the energy wells are infinitely narrow and the energy barrier is formally infinite. In the RHS model the energy wells have a finite curvature however the spinodal region is reduced to a single point. To study stability, we first remove these singularities by considering smoother potentials and then perform the appropriate limiting transition.

We start with the more general RHS model and regularize the bistable potential $u_{\rm RHS}$ by introducing an extended spinodal interval $[l-\epsilon; l+\epsilon]$ where the new potential $\tilde{u}_{\rm RHS}$ is concave. Assume that outside this interval the potential $\tilde{u}_{\rm RHS}$ coincides with $u_{\rm RHS}$ and is therefore convex. In a hard device the new RHS energy can be written in the form

$$v(\boldsymbol{x}, y; z) = \frac{1}{N}\sum_{i=1}^{N}\left[\tilde{u}_{\rm RHS}(x_i) + \frac{1}{2}(y-x_i)^2\right] + \frac{\lambda_f}{2}(z-y)^2. \tag{A1}$$

We now analyze stability of the system described by energy (A1). At a given z, the equilibrium equations can be written as

$$\frac{\partial v}{\partial x_i} = \tilde{u}'_{\rm RHS}(x_i) + (x - \hat{y}) = 0, \quad i = 1, \dots, N, \tag{A2}$$

where $\hat{y}(z, p, q, r)$ is the equilibrium value of y for a given configuration (p, q, r) given by Eq. 14. Assume that within the spinodal region there is an interval where $\tilde{u}''_{\rm RHS}(x)' < -1$. Then each of the equations (A2) has up to 3 solutions. We denote these solution by $\hat{x}_1(z, p, q, r), \hat{x}_0(z, p, q, r)$ and $\hat{x}_\star(z, p, q, r)$. The first two solutions $\hat{x}_1$ and $\hat{x_0}$ correspond to the two convex wells of the potential $\tilde{u}_{\rm RHS}(x)$ so that $\hat{x}_1 < l-\epsilon$ and $\hat{x}_0 > l+\epsilon$. The third solution $\hat{x}_\star$ describes the cross-bridge in the spinodal region and therefore $l - \epsilon \le \hat{x}_* \le l + \epsilon$ for all $\epsilon > 0$. We can now compute

$$\begin{aligned}
\left.\frac{\partial^2 v(\boldsymbol{x}, y, z)}{\partial x_i^2}\right|_{p,q,r,x_i=\hat{x}_1, y=\hat{y}, x_{j\neq i}=\hat{x}_j} &= \kappa_1 + 1 \equiv h_1 > 0,\\
\left.\frac{\partial^2 v(\boldsymbol{x}, y, z)}{\partial x_i^2}\right|_{p,q,r,x_i=\hat{x}_*, y=\overline{y}, x_{j\neq i}=\hat{x}_j} &= \tilde{u}''_{\rm RHS}(\hat{x}_*) + 1\\
&\equiv h_*(z, p, q, r) < 0,\\
\left.\frac{\partial^2 v(\boldsymbol{x}, y, z)}{\partial x_i^2}\right|_{p,q,r,x_i=\hat{x}_0, y=\hat{y}, x_{j\neq i}=\hat{x}_j} &= \kappa_0 + 1 \equiv h_0 > 0.
\end{aligned}$$

Here h_* is negative because the corresponding cross-bridge is the spinodal state. The other second derivatives of the energy can be computed explicitly

$$\begin{aligned}
\left.\frac{\partial^2 v(\boldsymbol{x}, y, z)}{\partial x_i \partial x_j}\right|_{p,q,r,x_i=\hat{x}_i, x_j=\hat{x}_j, x_{k\neq i,j}=\hat{x}_k, y=\hat{y}} &= 0 \text{ for } i \neq j,\\
\left.\frac{\partial^2 v(\boldsymbol{x}, y, z)}{\partial x_i \partial y}\right|_{p,q,r,x_i=\hat{x}_i, x_{j\neq i}=\hat{x}_j, y=\hat{y}} &= -1, \quad i = 1, \dots, N,\\
\left.\frac{\partial^2 v(\boldsymbol{x}, y, z)}{\partial y^2}\right|_{p,q,r,x_i=\hat{x}_i, y=\hat{y}} &= 1 + \lambda_f.
\end{aligned} \tag{A3}$$

To write the expression for the Hessian matrix $\mathbf{H}(z, p, q, r)$, it is convenient to introduce the following auxiliary quantities

$$H_i(z, p, q, r) = \left.\frac{\partial^2 v(\boldsymbol{x}, y, z)}{\partial x_i^2}\right|_{p,q,r,x_i=\hat{x}_i, y=\hat{y}, x_{j\neq i}=\hat{x}_j}.$$

Each of the variables H_i can take three values: h_1, h_0 and $h^\star$. Now we can write

$$\mathbf{H}(z, p, q, r) = \begin{pmatrix} H_1 & 0 & \cdots & 0 & -1 \\ 0 & \ddots & \ddots & \vdots & \vdots \\ \vdots & \ddots & \ddots & 0 & \vdots \\ 0 & \cdots & 0 & H_N & -1 \\ -1 & \cdots\cdots & & -1 & 1+\lambda_f \end{pmatrix}. \tag{A4}$$

To obtain a similar Hessian matrix for the HS model, we need to perform the limit $\kappa_{1,0}(z) \to \infty$ which means $h_1 \to \infty$, $h_0 \to \infty$ and $h_* \to -\infty$, and to drop in (A4) the last line and the last column.

From the form of the matrix $\mathbf{H}$, one can see that as soon as one of the terms H_i is equal to $h^\star(z)$, which means that $q > 0$, at least one of the principal minors of $\mathbf{H}$ becomes negative. This means that the absence of cross-bridges in the spinodal region is mandatory for stability at $\epsilon > 0$.

We can now consider the limit $\epsilon \to 0$. The value of the equilibrium strain in the spinodal region $\hat{x}_*$ remains between $l-\epsilon$ and $l+\epsilon$ and thus converges to l, when $\epsilon \to 0$. Therefore, if $q \neq 0$, the configuration (p, q, r) is necessary unstable and we know that such configurations are necessarily singular. Hence, in our RHS model, among the $(N+1)(N+2)/2$ equilibrium branches, $N(N+1)/2$ singular branches are unstable which leaves $N+1$ non-singular branches describing local minima of the energy. Since in the HS model the spinodal states are absent, all configurations are automatically metastable.

In the soft device case, the tension t is fixed while z becomes an additional degree of freedom. Then the energy of the nonsingular RHS system reads

$$w(\boldsymbol{x}, y, z; t) = \frac{1}{N}\sum_{i=1}^{N}\left[\tilde{u}_{\rm RHS}(x_i) + \frac{1}{2}(y-x_i)^2\right] + \frac{\lambda_f}{2}(z-y)^2 - tz. \tag{A5}$$

The analysis of the equilibrium states remains the same and we can similarly define the diagonal terms of the Hessian matrix for the energy $w(\boldsymbol{x}, y, z; t)$,

$$H_i(t,p,q,r) = \left.\frac{\partial^2 w(\boldsymbol{x},y,z,t)}{\partial x_i^2}\right|_{p,q,r,x_i=\hat{x}_i,y=\hat{y},z=\hat{z},x_{j\neq i}=\hat{x}_j}.$$

Here each term can take the following three values $h_1 = \kappa_1 + 1 > 0$, $h_0(p,q,r,t) = \kappa_0 + 1 > 0$ or $h^\star(p,q,r,t) < 0$. The other entries are the same as in the hard device case, see Eq. A3 except that now we have one additional row and one additional column,

$$\begin{aligned}
&\left.\frac{\partial^2 w(\boldsymbol{x},y,z,t)}{\partial x_i \partial z}\right|_{p,q,r,x_i=\hat{x}_i,x_{j\neq i}=\hat{x}_j,y=\hat{y},z=t,\hat{p},q,r} = 0,\\
&\quad \text{for } i = 1,\ldots,N\\
&\left.\frac{\partial^2 w(\boldsymbol{x},y,z,t)}{\partial y \partial z}\right|_{p,q,r,x_i=\hat{x}_i,x_{j\neq i}=\hat{x}_j,y=\hat{y},z=\hat{z}} = -\lambda_f,\\
&\left.\frac{\partial^2 w(\boldsymbol{x},y,z,t)}{\partial z^2}\right|_{p,q,r,x_i=\hat{x}_i,x_{j\neq i}=\hat{x}_j,y=\hat{y},z=\hat{z}} = \lambda_f.
\end{aligned}$$

By bringing all these second derivatives together we can write the Hessian matrix for the RHS model in a soft device

$$\mathbf{H}(z,p,q,r) = \begin{pmatrix}
H_1 & 0 & \cdots & 0 & -1 & 0\\
0 & \ddots & \ddots & \vdots & \vdots & \vdots\\
\vdots & \ddots & \ddots & 0 & \vdots & \vdots\\
0 & \cdots & 0 & H_N & -1 & 0\\
-1 & \ldots\ldots & -1 & (1+\lambda_f) & -\lambda_f\\
0 & \ldots\ldots & 0 & -\lambda_f & \lambda_f
\end{pmatrix}.$$

A straightforward adaptation of the above analysis shows that, as in a hard device, the system in a soft device is unstable only when $q \neq 0$, *i.e.* when at least one cross-bridge is in the spinodal state.

Finally, to obtain the Hessian matrix for the HS system we need to drop the last row and the last column and consider the limit $\kappa_{1,0}(z) \to \infty$ which means $h_1 \to \infty$, $h_0 \to \infty$ and $h_* \to -\infty$. We also require that $\lambda_f \to 0$. Then, the Hessian reads

$$\mathbf{H}_{HS}(z,p,q,r) = \begin{pmatrix}
H_1 & 0 & \cdots & 0 & -1\\
0 & \ddots & \ddots & \vdots & \vdots\\
\vdots & \ddots & \ddots & 0 & \vdots\\
0 & \cdots & 0 & H_N & -1\\
-1 & \ldots\ldots & -1 & 1
\end{pmatrix}.$$

The analysis here is similar to the case of a hard device and the conclusion is that again all equilibrium configurations are metastable.

[1] M. J. Buehler, S. Keten, and T. Ackbarow, Progress in Materials Science (2008).
[2] P. Fratzl, J. R. Soc. Interface **4**, 637 (2007).
[3] S. Suresh, Acta Materialia **55**, 3989 (2007).
[4] J. Howard, *Mechanics of Motor Proteins and the Cytoskeleton*, edited by Sinauer (Sinauer, Sunderland, MA, 2001).
[5] P. Nelson, *Biological Physics*, Energy, Information, Life (W. H. Freeman, 2003).
[6] Y. C. Fung, *Biomechanics*, Mechanical Properties of Living Tissues (Springer, 2010).
[7] R. C. Woledge, N. A. Curtin, and E. Homsher, Monogr Physiol Soc **41**, 1 (1985).
[8] M. Caruel, J.-M. Allain, and L. Truskinovsky, In preparation ().
[9] M. Caruel, J.-M. Allain, and L. Truskinovsky, In preparation ().
[10] A. F. Huxley, Prog. Biophys. Molec. Biol. **7**, 258 (1957).
[11] B. Alberts, A. Johnson, J. Lewis, M. Raff, K. Roberts, and P. Walter, *Molecular Biology of the Cell*, 5th ed. (2007).
[12] J. Howard, *Mechanics of motor proteins and the cytoskeleton*, edited by Sinauer (Sinauer, 2001).
[13] R. Lymn and E. Taylor, Biochemistry **10**, 4617 (1971).
[14] M. Linari, M. Caremani, and V. Lombardi, P Roy. Soc. Lond. B Bio. **277**, 19 (2010).
[15] K. Holmes and M. Geeves, Philos. T. Roy. Soc. B **355**, 419 (2000).
[16] T. A. McMahon, "Muscles, Reflexes, and Locomotion," Princeton University Press (1984).
[17] A. F. Huxley and R. M. Simmons, Nature **233**, 533 (1971).
[18] G. Piazzesi, M. Reconditi, M. Linari, L. Lucii, Y. Sun, T. Narayanan, P. Boesecke, V. Lombardi, and M. Irving, Nature **415**, 659 (2002).
[19] M. Reconditi, M. Linari, L. Lucii, A. Stewart, Y. Sun, P. Boesecke, T. Narayanan, R. Fischetti, T. Irving, G. Piazzesi, M. Irving, and V. Lombardi, Nature **428**, 578 (2004).
[20] M. Civan and R. Podolsky, Biophys. J. **184**, 511 (1966).
[21] H. Granzier, A. Mattiazzi, and G. Pollack, Am. J. Physiol. **259**, C266 (1990).
[22] G. Piazzesi, L. Lucii, and V. Lombardi, J. Physiol. - London **545**, 145 (2002).
[23] C. F. Armstrong, A. F. Huxley, and F. J. Julian, J. Physiol. **186**, 26P (1966).
[24] H. Sugi and T. Tsuchiya, J. Physiol. - London **319**, 219 (1981).
[25] K. A. P. Edman, J. Physiol. - London **404**, 301 (1988).
[26] K. A. P. Edman and N. Curtin, J. Physiol. - London **534**, 553 (2001).
[27] V. Decostre, P. Bianco, V. Lombardi, and G. Piazzesi, Proc. Natl. Acad. Sci. USA **102**, 13927 (2005).
[28] L. E. Ford, A. F. Huxley, and R. M. Simmons, J. Physiol.

269, 441 (1977).
[29] G. Piazzesi, F. Francini, M. Linari, and V. Lombardi, J. Physiol. **445**, 659 (1992).
[30] G. Piazzesi, M. Reconditi, M. Linari, L. Lucii, P. Bianco, E. Brunello, V. Decostre, A. Stewart, D. B. Gore, T. C. Irving, M. Irving, and V. Lombardi, Cell **131**, 784 (2007).
[31] M. Linari, G. Piazzesi, and V. Lombardi, Biophys. J. **96**, 583 (2009).
[32] G. Piazzesi, F. Francini, M. Linari, and V. Lombardi, J. Physiol. - London **445**, 659 (1992).
[33] G. I. Zahalak, Mathematical Biosciences **55**, 89 (1981).
[34] J. Sainte-Marie, D. Chapelle, R. Cimrman, and M. Sorine, Computers & Structures **84**, 1743 (2006).
[35] G. Piazzesi and V. Lombardi, Biophys. J. **68**, 1966 (1995).
[36] D. Smith, M. Geeves, J. Sleep, and S. Mijailovich, Ann. Biomed. Eng. **36**, 1624 (2008).
[37] D. Smith and M. S M, Ann. Biomed. Eng. **36**, 1353 (2008).
[38] F. Jülicher, A. Ajdari, and J. Prost, Rev. Mod. Phys. **69**, 1269 (1997).
[39] T. A. J. Duke, Proc. Natl. Acad. Sci. USA **96**, 2770 (1999).
[40] T. Duke, Philos. T. Roy. Soc. B **355**, 529 (2000).
[41] T. Guerin, J. Prost, and J. F. Joanny, Eur. Phys. J. **34**, 60 (2011).
[42] J. Liphardt, B. Onoa, S. B. Smith, I. Tinoco, and C. Bustamante, Science **292**, 733 (2001).
[43] A. N. Gupta, A. Vincent, K. Neupane, H. Yu, F. Wang, and M. T. Woodside, Nature Publishing Group **7**, 631 (2011).
[44] A. Prados, A. Carpio, and L. L. Bonilla, Phys. Rev. E **86**, 021919 (2012).
[45] G. Bell, Science **200** (1978).
[46] T. L. Hill, Prog. Biophys. Molec. Biol. **28**, 267 (1974).
[47] T. L. Hill, Prog. Biophys. Molec. Biol. **29**, 105 (1976).
[48] T. Erdmann and U. Schwarz, Phys. Rev. Lett. **108**, 188101 (2012).
[49] E. Eisenberg and T. Hill, Prog. Biophys. Molec. Biol. **33**, 55 (1978).
[50] L. Marcucci and L. Truskinovsky, Phys. Rev. E **81** (2010).
[51] L. Marcucci and L. Truskinovsky, Eur. Phys. J. E **32**, 411 (2010).
[52] B. DiDonna and A. Levine, Phys. Rev. E **75**, 041909 (2007).
[53] T. Erdmann, P. J. Albert, and U. S. Schwarz, J. Chem. Phys. **139**, 175104 (2013).
[54] H. Dietz and M. Rief, Phys. Rev. Lett. **100**, 098101 (2008).
[55] N. Thomas and Y. Imafuku, J Theor Biol (2012).
[56] K. Kometani and H. Shimizu, J. Stat. Phys. **13**, 473 (1975).
[57] R. C. Desai and R. Zwanzig, J. Stat. Phys. **19**, 1 (1978).
[58] L. E. Ford, A. F. Huxley, and R. M. Simmons, J. Physiol. - London **311**, 219 (1981).
[59] H. Huxley, A. Stewart, H. Sosa, and T. Irving, Biophys. J. **67**, 2411 (1994).
[60] K. Wakabayashi, Y. Sugimoto, H. Tanake, Y. Ueno, Y. Takezawa, and Y. Amemiya, Biophys. J. **67**, 2422 (1994).
[61] Z. G. Nicolaou and A. E. Motter, Nat Mater **11**, 608 (2012).
[62] A. Campa, T. Dauxois, and S. Ruffo, Physics Reports (2009).
[63] T. Erdmann and U. S. Schwarz, Eur. Phys. J. **22**, 123 (2007).
[64] T. Erdmann and U. S. Schwarz, Biophys. J. **91**, L60 (2006).
[65] T. Erdmann and U. S. Schwarz, Phys. Rev. Lett. **92**, 108102 (2004).
[66] H.-J. Lin, H.-Y. Chen, Y.-J. Sheng, and H.-K. Tsao, Phys. Rev. E **81** (2010).
[67] N. Bosaeus, A. H. El-Sagheer, T. Brown, S. B. Smith, B. Åkerman, C. Bustamante, and B. Nordén, Proc. Natl. Acad. Sci. U.S.A. **109**, 15179 (2012).
[68] V. Muñoz, E. R. Henry, J. Hofrichter, and W. A. Eaton, Proc. Natl. Acad. Sci. U.S.A. **95**, 5872 (1998).
[69] T. Bornschlögl and M. Rief, Physical Review Letters (2006).
[70] M. Caruel, J. M. Allain, and L. Truskinovsky, Phys. Rev. Lett. **110**, 248103 (2013).
[71] P.-G. de Gennes, C.R. Acad. Sci. IV-Phys. **2**, 1505 (2001).
[72] G. Puglisi and L. Truskinovsky, J. Mech. Phys. Solids (2005).
[73] G. Puglisi and L. Truskinovsky, J. Mech. Phys. Solids **48**, 1 (2000).
[74] J. M. Ball, Geometry, Mechanics, and Dynamics , 3 (2002).
[75] J. E. Cohen and P. Horowitz, Nature **352**, 699 (1991).
[76] M. T. Woodside, C. Garcia-Garcia, and S. M. Block, Curr. Opin. Chem. Biol. **12**, 640 (2008).
[77] A. Campa, S. Ruffo, and H. Touchette, Physica A **385**, 233 (2007).
[78] R. S. Ellis, J. Stat. Phys. **101**, 999 (2000).
[79] T. Dauxois, S. Lepri, and S. Ruffo, Commun. Nonlinear Sci. Numer. Simul. **8**, 375 (2003).
[80] F. Jülicher and J. Prost, Phys. Rev. Lett. **75**, 2618 (1995).
[81] T. Guerin, J. Prost, and J. F. Joanny, Phys. Rev. Lett. **104** (2010).
[82] S. Mijailovich, J. Fredberg, and J. Butler, Biophys. J. **71**, 1475 (1996).
[83] M. Linari, I. Dobbie, M. Reconditi, N. Koubassova, M. Irving, G. Piazzesi, and V. Lombardi, Biophys. J. **74**, 2459 (1998).
[84] F. Bouchet, S. Gupta, and D. Mukamel, Physica A **389**, 4389 (2010).
[85] Y. R. Efendiev and L. Truskinovsky, Continuum Mech. Therm. **22**, 679 (2010).
[86] B. Chen and H. Gao, Biophys. J. **101**, 396 (2011).
[87] H. Yao and H. Gao, J. Mech. Phys. Solids **54**, 1120 (2006).
[88] H. Gao, J. Qian, and B. Chen, J. R. Soc. Interface **8**, 1217 (2011).
[89] F. Jülicher and J. Prost, Phys. Rev. Lett. **78**, 4510 (1997).
[90] A. Srivastava and R. Granek, Phys. Rev. Lett. **110**, 138101 (2013).
[91] U. Gerland, R. Bundschuh, and T. Hwa, Biophysj **84**, 2831 (2003).
[92] B. Yurke, A. J. Turberfield, A. P. Mills, and F. C. Simmel, Nature (2000).